Retrospective Adversarial Replay for Continual Learning

Lilly Kumari
University of Washington
lkumari@uw.edu

Shengjie Wang
ByteDance
wsjloomise@gmail.com

Tianyi Zhou
University of Maryland
zhou@umiacs.umd.edu

Jeff Bilmes
University of Washington
bilmes@uw.edu

Abstract

Continual learning is an emerging research challenge in machine learning that addresses the problem where models quickly fit the most recently trained-on data and are prone to catastrophic forgetting due to distribution shifts — it does this by maintaining a small historical replay buffer in replay-based methods. To avoid these problems, this paper proposes a method, "Retrospective Adversarial Replay (RAR)", that synthesizes adversarial samples near the forgetting boundary. RAR perturbs a buffered sample towards its nearest neighbor drawn from the current task in a latent representation space. By replaying such samples, we are able to refine the boundary between previous and current tasks, hence combating forgetting and reducing bias towards the current task. To mitigate the severity of a small replay buffer, we develop a novel MixUp-based strategy to increase replay variation by replaying mixed augmentations. Combined with RAR, this achieves a holistic framework that helps to alleviate catastrophic forgetting. We show that this excels on broadly-used benchmarks and outperforms other continual learning baselines especially when only a small buffer is used. We conduct a thorough ablation study over each key component as well as a hyperparameter sensitivity analysis to demonstrate the effectiveness and robustness of RAR.

1 Introduction

Traditional supervised machine learning methods often rely on the assumption that the data is drawn i.i.d. from a stationary probability distribution. This assumption does not hold in many practical scenarios where the learner must continuously learn online and adapt to new tasks without revisiting previous tasks (and those tasks' data). This has motivated research in Continual Learning (also referred to as Lifelong Learning and Incremental Learning), where a machine learning model learns from a stream of data coming from a succession of different tasks [29, 45, 66].

The primary challenge in continual learning (CL) is to alleviate the "catastrophic forgetting" of the previously learnt tasks after learning new tasks [18, 39, 49]. This is mainly caused by a shift in the distribution of inputs and labels over time. For example, as a model is updated using new-task gradients, the hidden-layer representations, encoding information about previous tasks, become biased towards these new tasks. This leads to a model confusing the former with current tasks, thus producing incorrect predictions on older tasks. A widely studied strategy to alleviate forgetting is experience replay (ER) [10, 49, 50], which repeatedly trains the model on buffered replay data from previous tasks while learning the current task. However, the buffer in practice is often quite small [63], e.g., in autonomous driving, where the incremental data is large-scale and essentially never-ending. A model

36th Conference on Neural Information Processing Systems (NeurIPS 2022).

can thus over-fit to such small buffered data. Although forgetting is mitigated, the goal of retaining broad and accurate knowledge about previous tasks is not achieved, and the problem remains severe.

An ideal strategy to address the above challenge is to focus on the replay of "marginal samples" easier to forget and confuse with the current task's data, e.g., those near the boundary between the previous tasks' data and the current task's data. However, selecting such samples [2, 55] from a small buffer only brings limited improvement because the buffer (often formed using reservoir sampling [62] and thus is uniform) does not well cover many such marginal samples. Hence, we surmise that the core challenge is how to generate a small and sufficient set of samples, ones that are easier to forget and hence be confused with current task's data — given the limited buffer size, it is also important for these samples to be diverse and thus efficient.

In this paper, we propose a novel targeted adversarial synthesis based replay method, Retrospective Adversarial Replay (RAR), that can generate more informative replay instances with richer variations optimized to capture the forgetting frontier of continual learning, from a limited buffer. Specifically, given an incoming batch of the current task's data, RAR first identifies the most likely to be forgotten buffer samples (Stage I in Fig. 1) and pairs them with their nearest neighbors within the current task's data (Stage II in Fig. 1). For each pair, we then apply a bounded targeted adversarial perturbation to the buffer sample, which moves the buffer sample's hidden-layer representation towards that of the paired current task's sample (Stage III in Fig. 1). This three-step procedure, as illustrated in Fig. 1, generates fine-grained adversarial samples of the buffered data that capture "forgetting" at the local boundary to the current task's data. We then effectively reduce the risk of forgetting by replaying these perturbed samples. To improve the diversity and variation of the perturbed samples (thus increasing the information contained in a limited size buffer), we investigate the role of MixUp [58, 67, 68], a data augmentation technique applied together with RAR — we find that it brings substantial improvements when there are strict buffer size constraints.

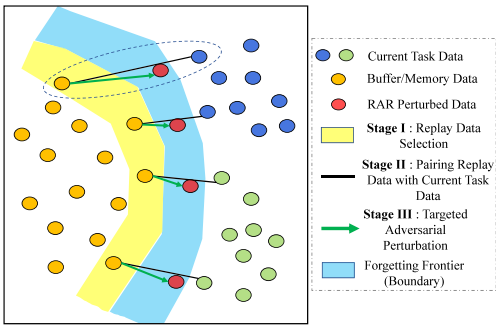

Figure 1: Our proposed RAR framework

For Stage I replay data selection, we utilize existing methods [2, 3, 10, 55, 65] resulting in an effective and data-efficient replay solution in CL, hence making RAR generic and complementary to existing memory-retrieval & update methods. Extensive experiments on RAR and comparisons to SoTA baselines from different CL categories demonstrate the advantages of RAR in reducing catastrophic forgetting and improving overall accuracy. Moreover, we conduct an ablation study showing that the key components such as replay samples selection strategy, sample pairing & adversarial perturbation, MixUp, etc, each bring appreciable improvements. Additional sensitivity analysis of the key hyperparameters implies that RAR is stable and consistently achieves these improvements.

Connection to human false memories & their correction: In human psychology, "false memories" [36, 42] refer to a wide variety of human memory errors ranging from the minor misremembering of small details (e.g., distorted recollection) all the way to unmitigated fabrication. The passage of time after experiencing an event increases the likelihood of these phenomena. They are referred to as [42] a "natural by-product of a distributed memory system (DMS)". Rather than a simple search & recollect, DMS [12] helps us in recombining and reconstructing memories via the integration of episodes from the past and present, but it is not always error-free. It is also true that when high-confidence false memories are corrected, people attend more to the provided feedback [17]. Despite a tendency for belief perseverance [4], the information that breaks through this perseverance is greatly attended to. The motivation behind RAR is in line with this theory. In RAR, we first combine/pair the replay buffer samples from previously seen tasks with the current data. Then using the pairing, we find existing high-confidence false memories in the form of targeted adversarial perturbations that are closer to the current data in the model's latent space. Finally, we provide the correct target for the perturbed input as feedback during the replay stage. On the other hand, existing ER-based CL methods lack this mechanism of combining past and present data and rely on simple retrieve and replay process.

2 Related Work

Existing approaches in CL can be broadly characterized into two groups based on the model's architecture. Methods dealing with *dynamic architecture* maintain separate parameters for each task [34, 53, 64]. These methods require the knowledge of task descriptors, are expensive to train and often do not scale well when dealing with a long sequence of online tasks. In this work, we focus on the *task-free setting of CL* [61]. *Fixed architecture* approaches use *regularization* techniques to selectively regularize parameters (either weights or outputs) important for old tasks [1, 8, 27, 32, 35, 52, 66], and require task information in general. This category also includes *memory-based* approaches for constrained parameter updates on new samples to minimize interference with previous tasks [9, 37] and for replaying them along with the new task's data [2, 3, 5, 6, 10, 13, 38, 41, 43, 44, 47, 48, 59, 55, 65]. Other ER methods [2, 51, 56, 60] train *generative models* on previous tasks which can be challenging owing to the online (single-pass) learning setting.

CL using Adversarial Information: ACL [16], belonging to the *dynamic architecture* category, uses adversarial learning to train a shared feature encoder and a discriminator using a GAN's minimax objective [19]. ASER [55] proposes using the kNN-specific Shapley value [24, 54] to select replay samples that are representative of the buffer and adversarially close to the decision boundaries of incoming classes. GMED [25] uses gradient updates to edit buffered samples individually based on their loss increase after a look-ahead update performed only on the incoming batch. Compared to these methods, RAR is a *fixed architecture task-free CL* framework that leverages the local pairwise relationships between the replay and current task's samples to locally perturb each replay sample in a targeted adversarial manner. Our targeted perturbation generates samples close to the forgetting frontier that are hence likely confusing for the model but that are also representative of previous data — this results in a good set to further train on. To elucidate the differences in detail, we also provide a more extensive survey of the relevant prior literature in Appendix B.

3 Retrospective Adversarial Replay

Formally, the continual learning problem consists of a stream of data distributions $(\mathcal{D}_1, \mathcal{D}_2, \ldots, \mathcal{D}_T)$ that corresponds to T tasks (in this work, the boundaries between tasks are not known). We get data points uniformly sampled from the data distribution of the current task. Our target is to train a machine learning model $f(\cdot;\theta)$ parameterized by θ that minimizes the losses as we learn each task in the given sequential order without increasing the loss on previously learned samples. In other words, the objective is

$$\min_{\theta} \sum_{i=1:T} \mathbb{E}_{(x,y)\sim\mathcal{D}_i} \ell(x, y; \theta) \tag{1}$$

Here, ℓ denotes the loss function and i is an index over the set of tasks. To retain the knowledge of previous tasks and mitigate catastrophic forgetting, similar to [2, 55, 65], we utilize a limited memory buffer to store samples representing previously seen data. Let $\mathcal{M}$ denote the memory/buffer, which is essentially a set of data points and $|\mathcal{M}| \leq m$. Similar to ER (Alg. 2), as we train on task i, we get an incoming batch $(X_i, Y_i) \sim D_i$, and we combine it with a subset of memory samples $(X'_M, Y'_M) \subset \mathcal{M}$ to compute the overall loss. We can then update the memory $\mathcal{M}$ by replacing some samples with the ones encountered in the current training step while keeping the size of the buffer unchanged.

In general, ER-based methods typically deal with two problems: (1) *Memory Update* for populating the buffer and (2) *Memory Retrieval* for selecting samples from the buffer for replay. In this work, we focus on synthesizing adversarial memory samples which provide the most conflicting information on the look-ahead probing step. In other words, the model trained only on the incoming task (one-step look-ahead) misclassifies the synthesized samples (anchored around previously seen classes stored in the memory) as the incoming classes. Thus, by learning on such adversarially synthesized memory samples in retrospect, we prevent any conflicts in the probing step. For problem (1), we use reservoir sampling to update the memory (Appendix C), which can give us uniform samples from the streaming data points and is widely adopted in many continual learning methods [2, 10, 55]. For problem (2), one can utilize any existing memory retrieval methods [2, 3, 10, 55, 65], thus making RAR complimentary and easily integratable with many existing CL methods.

3.1 Retrospective Adversarial Perturbation

Existing methods addressing the memory-retrieval problem optimize the model parameters using ℓ_{ER} in Eq. 2 where (X'_M, Y'_M) are selected from the buffer $\mathcal{M}$ based on their proposed selection strategies. For the ease of notation, we use $y(x)$ to denote the ground-truth label of sample x.

$$\ell_{ER}(X'_M, X_i, \theta) := \ell(X_i, y(X_i); \theta) + \ell(X'_M, y(X'_M); \theta) \tag{2}$$

ER [10] uses naive random sampling to select X'_M, GSS [3] encourages gradient diversity while sampling X'_M, ASER [55] uses kNN Shapley value to select samples which are representative of $\mathcal{M}$ and close to the samples in X_i in the latent space, and MIR [2] selects replay samples which are maximally interfered/forgotten after the look-ahead probing step. In the look-ahead probing step, the model is updated only on the incoming task samples such that $\theta' = \theta - \eta \nabla_\theta \ell(X_i, y(X_i); \theta)$.

Although the methods mentioned above cover crucial aspects (diversity, representativeness, similarity to incoming batch) for selecting X'_M, they do not capture the local pairwise interactions between the memory and current-task samples. Motivated by this, Retrospective Adversarial Replay Loss (ℓ_{RAR}) finds a cardinality-constrained pairing (E) between memory and incoming task samples such that the loss on memory samples that are perturbed towards the paired current-task samples is maximum:

$$\ell_{RAR}(X_M \times X_i, \theta, \theta') := \max_{\substack{E \subset X_M \times X_i \\ |E| = c}} \sum_{(x_M, x_i) \in E} \ell(g_{\theta'_l}(x_M, x_i), y(x_M); \theta) \tag{3}$$

Here, X_M denotes the entire input samples present in $\mathcal{M}$, and $g_{\theta'_l}(x_M, x_i)$ described mathematically in Eq. 4 can be seen as a targeted perturbation of x_M that is visually similar to x_M but close to the latent embedding of target $x_i \in X_i$ in the l-th layer latent space modeled by θ'. Since the min-objective in Eq. 4 aims to move the perturbed replay sample close to the current-task sample, $y(x_M) \neq y(x_i)$ for a particular pairing to be considered and to filter out any trivial pairings while optimizing Eq. 3.

$$g_{\theta'_l}(x_M, x_i) = \underset{z}{\operatorname{argmin}}\, d_{\theta'_l}(z, x_i) \;\; \text{s.t.} \; ||z - x_M||_\infty \leq \epsilon \tag{4}$$

$$\text{where } d_{\theta'_l}(z, x_i) := ||\theta'_l(z) - \theta'_l(x_i)||_2 \tag{5}$$

Since x_M and x_i have different labels, such perturbed samples that we get from Eq. 4 are confusing to the continual learner in terms of distinguishability from the current-task sample x_i, while still representing previous tasks based on their visual similarity to $x_M \in \mathcal{M}$. Eq. 3 essentially helps in the synthesis of targeted adversarial samples that are close to incoming samples X_i in the latent space and hence the learner will miss making the correct prediction $y(X_M)$ despite the fact that the adversarial samples are anchored around the original memory samples X_M. Training on such samples can help the model to learn about the boundaries between previous and current tasks and also retain the knowledge of previous tasks [7, 11, 23]. Note that the perturbations are performed based on the look-ahead parameters θ'. In other words, assuming we only learn from the current-task samples X_i and update the parameters to θ', the generated adversarial samples give us many training samples that show conflicting behaviors on θ' and get easily forgotten by the model. In retrospect, we can potentially prevent such forgetting when we are still at θ by using those targeted adversarial samples as training signals, i.e., we minimize the RAR loss (Eq. 3) to update the model θ.

Optimizing Eq. 3 over all feasible pairs of X_M and X_i is computationally challenging as we effectively need to compute the adversarial perturbations on all such pairs to select the most confusing subset incurring the maximum RAR loss. Moreover, each adversarial sample synthesis (Eq. 4) requires multiple gradient steps as we need to run adversarial attack algorithms such as the iterative-FGSM [15, 20] covered in detail in Appendix H. Thus, to eliminate this bottleneck, we propose two pruning strategies covered in sections 3.2 and 3.3 to reduce the candidate anchor-target pairs in $X_M \times X_i$ for adversarial perturbations and approximately optimize Eq. 3.

3.2 Selecting Replay Data from Buffer

To reduce the computational overhead, we only consider a subset of the memory buffer $X'_M \subset \mathcal{M}$ instead of considering all memory input samples X_M. Memory-retrieval methods such as ER [10], GSS [3], ASER [55], and MIR [2] can be used to select a smaller replay set X'_M. This again reiterates that RAR is generic and complementary to existing memory-retrieval methods.

3.3 Pairing between Buffer and Current-task Data

To further bring down the computational costs of adversarial perturbations, we perform another pruning over the possible pairs between $X'_M \times X_i$ based on samples' hidden representations. I.e., we first compute the distance $d_{\theta'_l}(x'_M, x_i)$, which is essentially the target value for the adversarial perturbation (Eq. 4) for every pair $(x'_M, x_i) \in X'_M \times X_i$ with different labels $y(x'_M) \neq y(x_i)$ and then screen out the pairs with larger distance values, maintaining only the smaller-distance ones, in accordance with the min-objective of Eq. 4. To utilize the information from the selected memory samples, we pair each $x'_M \in X'_M$ with its nearest neighbor with a different class/label in the incoming batch X_i of current task. Nearest-neighbor-based matched pairs already represent the most confusing samples as the samples in a pair belong to different classes. Thus, it is easier for the optimization procedure approximating Eq. 4 to further reduce the distances between pairs coming from different classes (shown in Fig. 2b), aiding in the synthesis of even more confusing adversarial samples.

Computational overhead for optimizing Eq. 3: First, we select memory samples for replay X'_M (Sec. 3.2) which has the same costs as the backbone memory-retrieval method. Next, we compute the distances between latent features of X'_M and incoming batch X_i with computational complexity of $\mathcal{O}(|X'_M| * |X_i|)$. This is minimal given the online nature of CL where the training batch size is often set to 10. After performing the nearest neighbor matching, we optimize Eq. 4 via iterative-FGSM [15] which introduces some additional computational costs, but we keep it marginal by using only two steps of iterative-FGSM. We provide further details in Appendix E and H.

Combining our RAR loss with the loss on selected memory samples and incoming batch samples, we have our overall objective (similar to Eq. 2) defined as follows, where β is a hyperparameter to control the trade-offs between the losses on original and adversarially synthesized memory samples.

$$\ell_{all}(X'_M, X_i, \theta) := \ell(X_i, y(X_i); \theta) + \beta \ell_{RAR}(X'_M \times X_i, \theta, \theta') + (1-\beta)\ell(X'_M, y(X'_M); \theta) \quad (6)$$

Algorithm 1 RAR - Retrospective Adversarial Replay for Continual Learning

1: **Input:** Tasks $(\mathcal{D}_1, \mathcal{D}_2, \ldots \mathcal{D}_T)$, Model θ, Learning Rate η, Memory $\mathcal{M}$, Memory Size m, Replay Budget k, Trade-off Parameter β, Perturbation Strength ϵ & number of gradient steps n
2: **Output:** Model θ
3: **for** task $i \in [T]$ **do**
4: **for** $(X_i, Y_i) \sim \mathcal{D}_i$ **do**
5: $\theta^{'} \leftarrow \text{SGD}(\ell(X_i, Y_i; \theta), \theta, \eta)$ { // Look-ahead update of model parameters}
6: Select (X'_M, Y'_M) from $\mathcal{M}$ s.t. $|X'_M| = k$ { // using existing memory-retrieval methods}
7: Let $S := \emptyset$
8: **for** $x'_M \in X'_M$ **do**
9: $x'_i \in \text{argmin}_{x_i \in X_i, y(x'_M) \neq y(x_i)} \, d_{\theta'_l}(x'_M, x_i)$
10: $S \leftarrow S \cup \{(x'_M, x'_i)\}$
11: **end for**
12: $\ell_{RAR}(S, \theta, \theta') \leftarrow \sum_{(x'_M, x_i) \in S} \ell(g_{\theta'_l}(x'_M, x_i), y(x'_M); \theta)$ { // perform the targeted adversarial perturbations (Appendix H) and define the corresponding RAR loss}
13: $\ell_{all} \leftarrow \ell(X_i, Y_i; \theta) + \beta \, \ell_{RAR}(S, \theta, \theta') + (1-\beta) \, \ell(X'_M, Y'_M; \theta)$
14: $\theta \leftarrow \text{SGD}(\ell_{all}, \theta, \eta)$
15: $\mathcal{M} \leftarrow \text{ReservoirUpdate}(X_i, Y_i, \mathcal{M}, m)$
16: **end for**
17: **end for**

Description of RAR framework: In Alg. 1, we describe our retrospective adversarial replay algorithm for continual learning. The algorithm essentially consists of three steps: (1) in Lines 5-6, we first perform the look-ahead parameter probing using the incoming samples of the current task to get θ', and select the subset X'_M using existing memory retrieval methods, such as ER, MIR, ASER, etc. (2) in Lines 7-11, we prune down the pairings between X'_M and X_i based on distances between hidden representations computed using Eq. 5, and (3) in Line 12, we define the RAR loss by performing adversarial perturbations on the selected pairs S. Note that since we use the selected pairings S of size k as an approximation of the true maximum-valued pairs, we can just sum over

entries in S instead of picking the maximum subset as done in Eq. 3. In Line 15, we update the memory buffer $\mathcal{M}$ based on incoming samples (X_i, Y_i) using reservoir sampling [62] and keep the memory limit m.

3.4 MixUp based Retrospective Adversarial Augmentation

We also propose another method *mix-RAR* utilizing the *mixup* technique [67] to bring in more diversity to the pool of replay examples selected from the buffer. After creating virtual examples $(\tilde{x}_M, \tilde{y}_M)$ using $x_i, x_j \in X'_M$ and $\lambda \in [0, 1]$ such that $\tilde{x}_M = \lambda x_i + (1-\lambda)x_j$ and $\tilde{y}_M = \lambda y_i + (1-\lambda)y_j$, we follow the original RAR algorithm to achieve pairing and subsequent targeted adversarial perturbation as shown in Alg 5 in Appendix A. The proposed MixUp strategy is different from [21, 40] as we apply mixup among the replay samples and then generate RAR perturbed samples anchored around them. This is positively coupled with RAR's objective. Given a current-task sample from class (c), training on an RAR perturbed sample generated using a mixup between two buffered samples from different past classes (a,b) can potentially help in capturing the forgetting frontier between three pairs of classes (a,c), (b,c) and (a,b), thus minimizing forgetting on both past classes.

4 Experiments

Datasets: We evaluate RAR on four supervised image classification benchmarks for task-free CL. **(1) Split-MNIST**[31] has five disjoint tasks, each having two classes. **(2) Split-CIFAR10** [28] consists 5 disjoint tasks with each task having two classes and 10k training examples. **(3) Split-CIFAR100** deals with 20 disjoint tasks with each task having 5 classes. **(4) Split-miniImageNet** [14] consists 20 disjoint tasks with each task having 5 classes and 2.5k training examples. We cover further statistics in Appendix D. All these datasets deal with the class-incremental scenario [61]. Our implementation code is available at https://github.com/lillykumari8/RAR-CL.

Table 1: Average Accuracy (↑) on different task-free CL datasets across different buffer sizes (m). We average results over 15 runs for all except for Split-MNIST where we average over 20 runs.

	Split-MNIST		Split-CIFAR10			Split-CIFAR100	Split-miniImageNet
Method	m=500	m=1000	m=200	m=500	m=1000	m=10,000	m=10,000
Fine-tuning	19.0 ± 0.2	19.0 ± 0.2	18.4 ± 0.3	18.4 ± 0.3	18.4 ± 0.3	3.06 ± 0.2	2.84 ± 0.4
AGEM	29.02 ± 5.3	-	22.7 ± 1.8	22.7 ± 1.9	22.6 ± 0.7	2.40 ± 0.2	2.92 ± 0.3
ER	80.7 ± 2.1	83.3 ± 1.4	25.7 ± 1.3	31.9 ± 0.9	39.5 ± 1.7	26.0 ± 0.3	23.7 ± 0.5
ER-RAR (ours)	$\mathbf{84.2 \pm 1.8}$	$\mathbf{86.9 \pm 1.1}$	$\mathbf{33.2 \pm 1.4}$	$\mathbf{40.4 \pm 1.7}$	$\mathbf{44.0 \pm 1.4}$	$\mathbf{29.8 \pm 0.4}$	$\mathbf{27.9 \pm 0.5}$
ER-mix	80.9 ± 1.3	81.7 ± 1.1	24.9 ± 1.8	33.0 ± 2.3	37.5 ± 1.6	26.6 ± 0.8	23.0 ± 1.1
ER-mix-RAR (ours)	$\mathbf{86.1 \pm 1.1}$	$\mathbf{86.9 \pm 1.0}$	$\mathbf{37.2 \pm 1.0}$	$\mathbf{41.6 \pm 1.0}$	$\mathbf{44.4 \pm 0.8}$	$\mathbf{31.5 \pm 0.6}$	$\mathbf{28.8 \pm 0.5}$
MIR	84.8 ± 1.2	86.3 ± 1.4	28.0 ± 1.5	37.5 ± 1.6	45.3 ± 1.2	26.7 ± 0.4	24.3 ± 0.6
MIR-RAR (ours)	$\mathbf{87.9 \pm 1.4}$	$\mathbf{89.4 \pm 1.1}$	$\mathbf{33.3 \pm 1.1}$	$\mathbf{43.1 \pm 1.1}$	$\mathbf{45.3 \pm 1.5}$	$\mathbf{29.3 \pm 0.4}$	$\mathbf{26.7 \pm 0.7}$
MIR-mix	85.7 ± 0.8	86.6 ± 0.7	35.2 ± 1.2	40.7 ± 0.8	42.5 ± 1.5	27.6 ± 0.5	23.3 ± 0.8
MIR-mix-RAR (ours)	$\mathbf{89.0 \pm 0.7}$	$\mathbf{89.1 \pm 1.0}$	$\mathbf{37.6 \pm 1.0}$	$\mathbf{42.9 \pm 1.1}$	$\mathbf{44.7 \pm 1.3}$	$\mathbf{29.9 \pm 0.4}$	$\mathbf{27.7 \pm 0.5}$
ASER	79.6 ± 2.5	79.5 ± 1.5	24.2 ± 1.2	32.2 ± 1.5	37.0 ± 2.3	26.5 ± 0.6	25.0 ± 0.8
ASER-RAR (ours)	$\mathbf{81.3 \pm 1.5}$	$\mathbf{83.2 \pm 1.1}$	$\mathbf{34.5 \pm 1.2}$	$\mathbf{40.4 \pm 1.0}$	$\mathbf{42.7 \pm 1.3}$	$\mathbf{29.5 \pm 0.4}$	$\mathbf{26.9 \pm 0.7}$
ASER-mix	80.2 ± 1.8	79.6 ± 1.7	25.9 ± 1.2	29.5 ± 1.8	34.0 ± 1.7	26.8 ± 0.6	22.1 ± 0.9
ASER-mix-RAR (ours)	$\mathbf{82.0 \pm 1.6}$	$\mathbf{84.0 \pm 1.2}$	$\mathbf{35.6 \pm 0.9}$	$\mathbf{39.2 \pm 1.4}$	$\mathbf{41.5 \pm 1.6}$	$\mathbf{29.9 \pm 0.3}$	$\mathbf{27.5 \pm 0.5}$
iid-online	86.8 ± 1.1	86.8 ± 1.1	60.8 ± 1.0	60.8 ± 1.0	60.8 ± 1.0	18.13 ± 0.8	17.53 ± 1.6
iid-offline	92.3 ± 0.5	92.3 ± 0.5	79.2 ± 0.4	79.2 ± 0.4	79.2 ± 0.4	42.0 ± 0.9	37.46 ± 1.3

Evaluation Metrics: Following [8, 37], we use two standard metrics used in CL to evaluate RAR's performance. *Final average accuracy (A_T)* assesses the overall performance of the model whereas *Final average forgetting (F_T)* measures how much the model has forgotten each task once the online learning has completed. Lower forgetting is better. Below, $a_{i,j}$ denotes the accuracy evaluated on the test set of task j after the model has experienced all tasks up to i.

$$A_T = \frac{1}{T}\sum_{j=1}^{T} a_{T,j} \quad F_T = \frac{1}{T-1}\sum_{j=1}^{T-1} \max_{l \in \{1,\ldots T-1\}} (a_{l,j} - a_{T,j}) \tag{7}$$

Settings and Hyperparameters: We follow the same setup as [2] for deciding model architectures for all four datasets. For Split-MNIST, we use an MLP classifier with two hidden layers, each with

Table 2: Average Forgetting (↓) on different task-free CL datasets across different buffer sizes (m). We average results over 15 runs for all except for Split-MNIST where we average over 20 runs.

	Split-MNIST		Split-CIFAR10			Split-CIFAR100	Split-miniImageNet
Method	m=500	m=1000	m=200	m=500	m=1000	m=10,000	m=10,000
ER	17.1 ± 2.6	13.1 ± 1.8	51.3 ± 4.1	39.0 ± 2.1	26.3 ± 2.4	17.1 ± 0.5	28.3 ± 0.6
ER-RAR (ours)	$\mathbf{11.0 \pm 2.5}$	$\mathbf{7.4 \pm 1.1}$	$\mathbf{37.6 \pm 2.1}$	$\mathbf{25.1 \pm 2.5}$	$\mathbf{18.1 \pm 2.0}$	$\mathbf{10.8 \pm 0.4}$	$\mathbf{16.4 \pm 0.8}$
ER-mix	17.3 ± 1.6	15.8 ± 1.5	54.9 ± 5.2	37.2 ± 3.5	25.8 ± 4.0	21.9 ± 1.1	33.9 ± 1.5
ER-mix-RAR (ours)	$\mathbf{9.6 \pm 1.4}$	$\mathbf{8.4 \pm 1.5}$	$\mathbf{27.4 \pm 2.3}$	$\mathbf{20.1 \pm 1.6}$	$\mathbf{15.4 \pm 1.1}$	$\mathbf{10.7 \pm 0.4}$	$\mathbf{16.5 \pm 1.1}$
MIR	10.7 ± 1.6	7.5 ± 1.8	48.1 ± 2.9	32.2 ± 2.1	19.1 ± 1.8	13.8 ± 0.4	21.4 ± 0.6
MIR-RAR (ours)	$\mathbf{6.1 \pm 1.2}$	$\mathbf{3.1 \pm 0.7}$	$\mathbf{33.5 \pm 2.2}$	$\mathbf{21.1 \pm 2.2}$	$\mathbf{14.1 \pm 1.6}$	$\mathbf{10.9 \pm 0.5}$	$\mathbf{15.5 \pm 0.8}$
MIR-mix	8.7 ± 0.9	7.8 ± 1.1	$\mathbf{24.7 \pm 2.6}$	$\mathbf{16.1 \pm 2.2}$	$\mathbf{12.9 \pm 2.7}$	16.4 ± 0.6	30.3 ± 1.2
MIR-mix-RAR (ours)	$\mathbf{4.6 \pm 1.0}$	$\mathbf{4.1 \pm 1.0}$	26.6 ± 1.9	17.4 ± 1.7	13.1 ± 2.0	$\mathbf{11.3 \pm 0.5}$	$\mathbf{13.7 \pm 1.0}$
ASER	19.1 ± 3.0	17.8 ± 2.4	64.3 ± 3.3	45.5 ± 3.3	29.3 ± 3.4	16.8 ± 0.6	27.0 ± 1.0
ASER-RAR (ours)	$\mathbf{15.4 \pm 2.2}$	$\mathbf{12.0 \pm 1.9}$	$\mathbf{35.4 \pm 2.0}$	$\mathbf{21.4 \pm 2.0}$	$\mathbf{14.5 \pm 1.6}$	$\mathbf{8.9 \pm 0.4}$	$\mathbf{15.9 \pm 1.0}$
ASER-mix	18.6 ± 2.2	18.9 ± 2.6	54.7 ± 3.8	50.1 ± 4.7	38.1 ± 3.3	21.7 ± 0.8	33.7 ± 1.0
ASER-mix-RAR (ours)	$\mathbf{16.1 \pm 2.3}$	$\mathbf{12.0 \pm 1.7}$	$\mathbf{30.3 \pm 1.8}$	$\mathbf{21.5 \pm 3.3}$	$\mathbf{18.7 \pm 3.2}$	$\mathbf{11.0 \pm 0.5}$	$\mathbf{12.4 \pm 1.0}$

400 units with ReLU activation, followed by a linear classifier layer with 10 units. For Split CIFAR-10, Split CIFAR-100, and Split mini-ImageNet, we use a reduced ResNet-18 classifier [22]. The replay budget k is the same as the mini-batch size (fixed to 10) irrespective of the buffer size m. For hyperparameters tuning on each dataset, we hold-out 5% of the training samples for each task and use it as a validation set. We provide additional details about the implementation settings in Appendix F.

4.1 Main Results

We report the average accuracy and forgetting in Table 1 and 2 respectively for experiments on all four datasets under various buffer size constraints. We use three different memory-retrieval methods, namely *ER* [10], *MIR* [2], and *ASER* [55] and compare *RAR* and *mix-RAR* with their respective baselines which do not use the RAR loss (Eq. 3). For fair comparison, we compare *mix-RAR* with baseline retrieval methods using mixup between replay samples. We also compare against standard baseline methods: (a) *Fine-tuning*, which trains the model continuously on the stream of tasks without employing any strategy to avoid forgetting, (b) *Averaged Gradient Episodic Memory (AGEM)* [9] (c) *iid-online*, which trains a model on the iid-data sampled from entire dataset $\mathcal{D} = \cup_{i=1}^{T} \mathcal{D}_i$ for a single epoch, (d) *iid-offline*, which trains a model similar to the iid-online setting but for multiple epochs (three epochs considered in the reported results). We compare against another memory sample perturbation method called *GMED* [25] in Table 3 to avoid repetition.

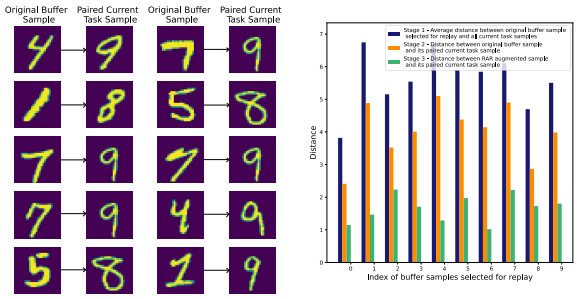

(a) (b)

Figure 2: Split-MNIST - (a) Buffer samples selected for replay using MIR strategy along with their paired current-task sample. (b) Visualization of how the distance between the buffered replay samples and its nearest neighbor in the current tasks' batch evolves across different stages of RAR

We provide the pseudo-code for ER (Alg. 2), ER-RAR (Alg. 3), MIR-RAR (Alg. 4), and mix-RAR (Alg. 5) in Appendix A to describe how our proposed framework can be unified with existing CL methods. Also, we leave out the results against GSS [3] as both MIR [2] and ASER [55] outperform it in terms of accuracy and forgetting. As shown in Table 1, both *RAR* and *mix-RAR* using different memory-retrieval methods consistently outperform their respective non-RAR baselines (without and with mixup) across all four datasets. From Table 2, we observe that the improvements obtained by integrating *RAR* with respective replay selection methods *{ER, MIR & ASER}* (both without and with mixup) are significant. In case of Split-CIFAR10, *MIR-mix* tends to perform slightly better than *MIR-mix-RAR* in terms of forgetting, but based on accuracy improvement that *MIR-mix-RAR* brings, the relative difference is negligible since forgetting is dependent on the maximum accuracy that a continual learner achieves across different tasks.

In the case of Split-miniImageNet, ER-mix-RAR method achieves the best average accuracy of 28.8%, outperforming other MIR & ASER based methods, and has similar observation on the Split-CIFAR100 dataset. We hypothesize that for large buffer sizes such as 10k (100 examples per

class), the ER-based selection aids in sampling a diverse set of classes from the memory buffer compared to MIR & ASER, thus improving the overall accuracy. However, since MIR & ASER consider samples suffering interference from the new task's data, MIR-mix-RAR & ASER-mix-RAR help minimize the forgetting on the old tasks.

The improved performance of ER-RAR, MIR-RAR, and ASER-RAR compared to ER, RAR, and ASER respectively demonstrates that RAR is able to alleviate catastrophic forgetting on old tasks via generating diverse and confusing samples close to the forgetting frontier. To ensure fair comparison in terms of computational costs, in Table 5 in Appendix I, we also compare RAR to GMED [25], ER-3-iters, and MIR-3-iters. 3-iters means that the model is trained for multiple iterations on the incoming batch and buffer samples as a new batch comes in.

Table 3: Comparison of RAR to other replay data perturbation methods: (a) Random edit using same perturbation tolerance as RAR (b) GMED. Numbers within bracket denote overall buffer size used.

	Split-MNIST (200)		**Split-CIFAR10 (200)**		**Split-CIFAR10 (500)**		**Split-CIFAR100 (10k)**	
Method	Accuracy	Forgetting	Accuracy	Forgetting	Accuracy	Forgetting	Accuracy	Forgetting
ER-Random	80.2 ± 2.3	18.7 ± 3.1	28.5 ± 1.6	41.9 ± 2.5	38.3 ± 1.1	30.2 ± 1.6	26.3 ± 0.5	14.4 ± 0.5
ER-GMED	82.5 ± 1.4	15.0 ± 1.7	30.4 ± 0.9	39.0 ± 1.3	38.3 ± 1.1	27.7 ± 1.3	25.5 ± 0.5	13.5 ± 0.5
ER-RAR (ours)	$\mathbf{84.0 \pm 1.1}$	$\mathbf{11.8 \pm 1.5}$	$\mathbf{33.2 \pm 1.4}$	$\mathbf{37.6 \pm 2.1}$	$\mathbf{40.4 \pm 1.7}$	$\mathbf{25.1 \pm 2.5}$	$\mathbf{29.8 \pm 0.4}$	$\mathbf{10.8 \pm 0.4}$
MIR-Random	82.3 ± 1.6	15.9 ± 1.7	29.1 ± 1.2	45.3 ± 2.4	39.2 ± 1.3	29.0 ± 2.1	26.5 ± 0.3	13.6 ± 0.5
MIR-GMED	84.2 ± 1.2	12.2 ± 1.0	27.5 ± 1.3	45.5 ± 1.6	37.2 ± 1.1	28.6 ± 1.9	25.1 ± 0.3	11.7 ± 0.4
MIR-RAR (ours)	$\mathbf{86.2 \pm 0.6}$	$\mathbf{9.1 \pm 0.8}$	$\mathbf{33.3 \pm 1.1}$	$\mathbf{33.5 \pm 2.2}$	$\mathbf{43.1 \pm 1.1}$	$\mathbf{21.1 \pm 2.2}$	$\mathbf{29.3 \pm 0.4}$	$\mathbf{10.9 \pm 0.5}$

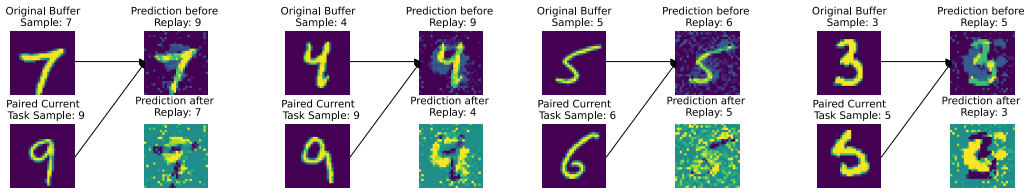

Figure 3: Retrospective Adversarial Perturbations (top-right of each sub-figure) for different replay samples shown along side original replay samples (top-left) and paired current-task sample (bottom-left). The bottom-right image shows the scaled perturbation that was added to the original buffered sample to generate the RAR perturbed data.

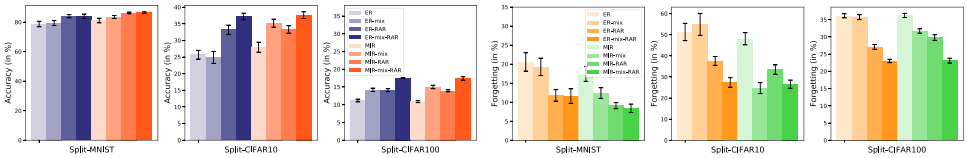

(a) Accuracy (↑) (b) Forgetting (↓)

Figure 4: Results under small buffer constraints, 20 examples per class for each dataset

Case study: Visualizing the Three Stages of RAR For the Split-MNIST dataset, we visually analyze the three stages of the RAR framework for a buffer size of 500 using MIR as the memory-retrieval method. Fig. 2a shows the samples selected for replay using the MIR score (Eq. 8) and their paired samples from the current task's batch based on distances computed using Eq. 5. Fig. 2b shows how the distance between a replaying sample and current task's data changes over the three stages: (1) for each sample selected from the buffer, the blue bar represents its average distance to all samples in the current-task batch; (2) after pairing each buffered replay sample with its nearest neighbor as described in Section 3.3, its distance to the paired sample (orange bar) becomes smaller than the blue bar; (3) after applying adversarial perturbations to each buffered sample as described in Section 3.1, the distance is further reduced. The decrease of distance indicates that the pairing and adversarial perturbation in RAR are effective in generating samples closer to the forgetting frontier than the original buffer data selected for replay, meaning the RAR perturbations are similar to X_M but very close to the paired samples in X_i (current task's batch) in the *l-th* layer latent representation space of model θ. In Fig. 3, we show four examples of RAR perturbed samples generated via Eq. 4 from four buffer samples and their paired samples from the current task. For most of the buffer samples, a single gradient step of θ

replaying them and their RAR perturbed counterparts suffices to correct their wrong predictions (e.g., the current task's classes), hence effectively alleviating the model's forgetting on previous tasks.

4.2 Advantage of MixUp in Small-Buffer Cases

On each dataset, as reported in Table 2, all mix-RAR methods perform better compared to RAR methods in terms of reducing forgetting on previous tasks with slight improvement in average accuracy. The proposed use of MixUp among the replay samples before RAR is able to increase the variation of RAR perturbed samples, which is essential to CL with a small buffer. To verify its effectiveness, we conduct experiments that store only 20 examples per class. Figure 4 shows that ER-mix-RAR & MIR-mix-RAR consistently outperform other ER & MIR methods respectively. We can achieve even more significant improvements in forgetting, particularly for more challenging tasks such as Split-CIFAR100.

4.3 Ablation Study to Verify the Effectiveness of RAR

In Table 3, we compare RAR methods to two baseline methods: (a) *Random* which add a perturbation of the same tolerance as the RAR method to the replay samples before the experience replay stage, (b) *GMED* [25] which performs smart gradient updates in the input space by treating each replay sample individually (no local pairing considered between buffer and current task's data). As can be seen in Table 3, ER-RAR and MIR-RAR consistently outperform other methods confirming RAR's superior ability to tackle catastrophic forgetting via generating targeted perturbations influenced by the local interference between different task's data.

4.4 Sensitivity Analysis of Hyperparameters

In Fig. 5, we plot the sensitivity of RAR's performance with respect to the number of gradient steps n used to generate the retrospective adversarial samples via optimizing Eq. 4 in the input space. For Split-CIFAR10 and Split-miniImageNet (where we report results using two gradient steps), we observe that for a larger number of steps $\{5, 10\}$, the performance stays comparable. This suggests that nearest-neighbor-based pairing using distance computations (covered in Sec 3.3) helps achieve anchor-target pairs which are already optimized and hence do not require numerous gradient updates to get classified as the paired target class from the current task.

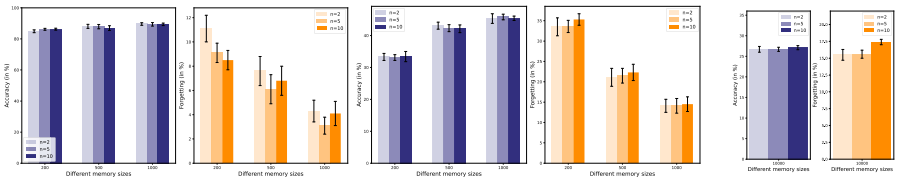

(a) Split-MNIST (b) Split-CIFAR10 (c) Split-miniImg

Figure 5: Sensitivity of the performance of RAR (using MIR) to number of perturbation steps (n) used to generate the RAR perturbed samples on different datasets under various buffer constraints.

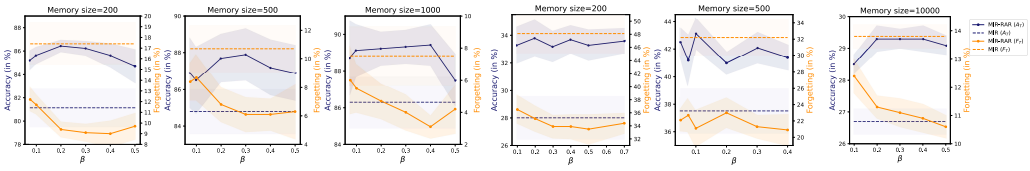

(a) Split-MNIST (b) Split-CIFAR10 (c) Split-CIFAR100

Figure 6: Sensitivity of the performance of RAR (using MIR) to the trade-off coefficient (β) dedicated to ℓ_{RAR} on different datasets under various buffer constraints.

Next, we study the sensitivity of RAR corresponding to β which denotes the trade-off coefficient associated with ℓ_{RAR} in the final loss objective Eq. 6 — we use only one coefficient to reduce hyperparameter search costs. Fig. 6 shows that RAR (using MIR) outperforms vanilla MIR in terms of both accuracy (solid blue line is always above the dashed blue line) and forgetting (solid orange line always stays below the dashed orange line) for various non-zero values of β across the studied datasets.

5 Conclusion

In this paper, we study how to perturb limited buffer replay data to mitigate catastrophic forgetting in continual learning. We propose "Retrospective Adversarial Replay (RAR)", which focuses on previous tasks' data near the forgetting boundary to the current task in the model's representation space. RAR first allocates the most confusing pairs of a buffered sample and a current task's sample and then applies a bounded targeted adversarial perturbation to the former, which further moves it towards the latter in the model's representation space and creates a perturbed sample close to the boundary. Moreover, we study the role of MixUp in increasing the variation of replay augmentations, which significantly improves CL in the small buffer regime. When integrated with existing replay methods, RAR consistently outperforms previous CL methods across benchmark datasets under different settings.

Acknowledgements

This work was supported in part by the CONIX Research Center, one of six centers in JUMP, a Semiconductor Research Corporation (SRC) program sponsored by DARPA. We would also like to thank the Melodi lab students: Arnav Das and Gantavya Bhatt for their useful discussions.

References

[1] Rahaf Aljundi, Francesca Babiloni, Mohamed Elhoseiny, Marcus Rohrbach, and Tinne Tuytelaars. Memory aware synapses: Learning what (not) to forget. In *Proceedings of the European Conference on Computer Vision (ECCV)*, pages 139–154, 2018.

[2] Rahaf Aljundi, Lucas Caccia, Eugene Belilovsky, Massimo Caccia, Min Lin, Laurent Charlin, and Tinne Tuytelaars. Online continual learning with maximally interfered retrieval. *arXiv preprint arXiv:1908.04742*, 2019.

[3] Rahaf Aljundi, Min Lin, Baptiste Goujaud, and Yoshua Bengio. Gradient based sample selection for online continual learning. *arXiv preprint arXiv:1903.08671*, 2019.

[4] Craig A Anderson, Mark R Lepper, and Lee Ross. Perseverance of social theories: The role of explanation in the persistence of discredited information. *Journal of personality and social psychology*, 39(6):1037, 1980.

[5] Zalán Borsos, Mojmir Mutny, and Andreas Krause. Coresets via bilevel optimization for continual learning and streaming. *Advances in Neural Information Processing Systems*, 33: 14879–14890, 2020.

[6] Pietro Buzzega, Matteo Boschini, Angelo Porrello, Davide Abati, and Simone Calderara. Dark experience for general continual learning: a strong, simple baseline. *Advances in neural information processing systems*, 33:15920–15930, 2020.

[7] Xiaoyu Cao and Neil Zhenqiang Gong. Mitigating evasion attacks to deep neural networks via region-based classification. In *Proceedings of the 33rd Annual Computer Security Applications Conference*, pages 278–287, 2017.

[8] Arslan Chaudhry, Puneet K Dokania, Thalaiyasingam Ajanthan, and Philip HS Torr. Riemannian walk for incremental learning: Understanding forgetting and intransigence. In *Proceedings of the European Conference on Computer Vision (ECCV)*, pages 532–547, 2018.

[9] Arslan Chaudhry, Marc'Aurelio Ranzato, Marcus Rohrbach, and Mohamed Elhoseiny. Efficient lifelong learning with a-gem. *arXiv preprint arXiv:1812.00420*, 2018.

[10] Arslan Chaudhry, Marcus Rohrbach, Mohamed Elhoseiny, Thalaiyasingam Ajanthan, Puneet K Dokania, Philip HS Torr, and Marc'Aurelio Ranzato. On tiny episodic memories in continual learning. *arXiv preprint arXiv:1902.10486*, 2019.

[11] Kanghyun Choi, Deokki Hong, Noseong Park, Youngsok Kim, and Jinho Lee. Qimera: Data-free quantization with synthetic boundary supporting samples. *Advances in Neural Information Processing Systems*, 34, 2021.

[12] Thomas B Christophel, P Christiaan Klink, Bernhard Spitzer, Pieter R Roelfsema, and John-Dylan Haynes. The distributed nature of working memory. *Trends in cognitive sciences*, 21(2): 111–124, 2017.

[13] Matthias De Lange and Tinne Tuytelaars. Continual prototype evolution: Learning online from non-stationary data streams. In *Proceedings of the IEEE/CVF International Conference on Computer Vision*, pages 8250–8259, 2021.

[14] Jia Deng, Wei Dong, Richard Socher, Li-Jia Li, Kai Li, and Li Fei-Fei. Imagenet: A large-scale hierarchical image database. In *2009 IEEE conference on computer vision and pattern recognition*, pages 248–255. Ieee, 2009.

[15] Yinpeng Dong, Fangzhou Liao, Tianyu Pang, Hang Su, Jun Zhu, Xiaolin Hu, and Jianguo Li. Boosting adversarial attacks with momentum. In *Proceedings of the IEEE conference on computer vision and pattern recognition*, pages 9185–9193, 2018.

[16] Sayna Ebrahimi, Franziska Meier, Roberto Calandra, Trevor Darrell, and Marcus Rohrbach. Adversarial continual learning. In *European Conference on Computer Vision*, pages 386–402. Springer, 2020.

[17] Lisa K Fazio and Elizabeth J Marsh. Correcting false memories. *Psychological science*, 21(6): 801–803, 2010.

[18] Robert M French. Catastrophic forgetting in connectionist networks. *Trends in cognitive sciences*, 3(4):128–135, 1999.

[19] Ian Goodfellow, Jean Pouget-Abadie, Mehdi Mirza, Bing Xu, David Warde-Farley, Sherjil Ozair, Aaron Courville, and Yoshua Bengio. Generative adversarial nets. *Advances in neural information processing systems*, 27, 2014.

[20] Ian J Goodfellow, Jonathon Shlens, and Christian Szegedy. Explaining and harnessing adversarial examples. *arXiv preprint arXiv:1412.6572*, 2014.

[21] Xuejun Han and Yuhong Guo. Continual learning with dual regularizations. In *Joint European Conference on Machine Learning and Knowledge Discovery in Databases*, pages 619–634. Springer, 2021.

[22] Kaiming He, Xiangyu Zhang, Shaoqing Ren, and Jian Sun. Deep residual learning for image recognition. In *Proceedings of the IEEE conference on computer vision and pattern recognition*, pages 770–778, 2016.

[23] Byeongho Heo, Minsik Lee, Sangdoo Yun, and Jin Young Choi. Knowledge distillation with adversarial samples supporting decision boundary. In *Proceedings of the AAAI Conference on Artificial Intelligence*, volume 33, pages 3771–3778, 2019.

[24] Ruoxi Jia, David Dao, Boxin Wang, Frances Ann Hubis, Nick Hynes, Nezihe Merve Gürel, Bo Li, Ce Zhang, Dawn Song, and Costas J Spanos. Towards efficient data valuation based on the shapley value. In *The 22nd International Conference on Artificial Intelligence and Statistics*, pages 1167–1176. PMLR, 2019.

[25] Xisen Jin, Arka Sadhu, Junyi Du, and Xiang Ren. Gradient-based editing of memory examples for online task-free continual learning. *Advances in Neural Information Processing Systems*, 34, 2021.

[26] Chris Dongjoo Kim, Jinseo Jeong, and Gunhee Kim. Imbalanced continual learning with partitioning reservoir sampling. In *European Conference on Computer Vision*, pages 411–428. Springer, 2020.

[27] James Kirkpatrick, Razvan Pascanu, Neil Rabinowitz, Joel Veness, Guillaume Desjardins, Andrei A Rusu, Kieran Milan, John Quan, Tiago Ramalho, Agnieszka Grabska-Barwinska, et al. Overcoming catastrophic forgetting in neural networks. *Proceedings of the national academy of sciences*, 114(13):3521–3526, 2017.

[28] Alex Krizhevsky, Geoffrey Hinton, et al. Learning multiple layers of features from tiny images. 2009.

[29] Abhishek Kumar and Hal Daumé. Learning task grouping and overlap in multi-task learning. In *Proceedings of the 29th International Coference on International Conference on Machine Learning*, ICML'12, page 1723–1730, 2012.

[30] Alexey Kurakin, Ian Goodfellow, Samy Bengio, et al. Adversarial examples in the physical world, 2016.

[31] Yann LeCun. The mnist database of handwritten digits. *http://yann. lecun. com/exdb/mnist/*, 1998.

[32] Sang-Woo Lee, Jin-Hwa Kim, Jaehyun Jun, Jung-Woo Ha, and Byoung-Tak Zhang. Overcoming catastrophic forgetting by incremental moment matching. *Advances in neural information processing systems*, 30, 2017.

[33] Soochan Lee, Junsoo Ha, Dongsu Zhang, and Gunhee Kim. A neural dirichlet process mixture model for task-free continual learning. *arXiv preprint arXiv:2001.00689*, 2020.

[34] Xilai Li, Yingbo Zhou, Tianfu Wu, Richard Socher, and Caiming Xiong. Learn to grow: A continual structure learning framework for overcoming catastrophic forgetting. In *International Conference on Machine Learning*, pages 3925–3934. PMLR, 2019.

[35] Zhizhong Li and Derek Hoiem. Learning without forgetting. *IEEE transactions on pattern analysis and machine intelligence*, 40(12):2935–2947, 2017.

[36] Elizabeth F Loftus and Jacqueline E Pickrell. The formation of false memories, 1995.

[37] David Lopez-Paz and Marc'Aurelio Ranzato. Gradient episodic memory for continual learning. *Advances in neural information processing systems*, 30:6467–6476, 2017.

[38] Zheda Mai, Ruiwen Li, Hyunwoo Kim, and Scott Sanner. Supervised contrastive replay: Revisiting the nearest class mean classifier in online class-incremental continual learning. In *Proceedings of the IEEE/CVF Conference on Computer Vision and Pattern Recognition*, pages 3589–3599, 2021.

[39] Michael McCloskey and Neal J Cohen. Catastrophic interference in connectionist networks: The sequential learning problem. In *Psychology of learning and motivation*, volume 24, pages 109–165. Elsevier, 1989.

[40] Fei Mi, Lingjing Kong, Tao Lin, Kaicheng Yu, and Boi Faltings. Generalized class incremental learning. In *Proceedings of the IEEE/CVF Conference on Computer Vision and Pattern Recognition Workshops*, pages 240–241, 2020.

[41] Seyed Iman Mirzadeh, Mehrdad Farajtabar, Razvan Pascanu, and Hassan Ghasemzadeh. Understanding the role of training regimes in continual learning. *Advances in Neural Information Processing Systems*, 33:7308–7320, 2020.

[42] Eryn J Newman and D Stephen Lindsay. False memories: What the hell are they for? *Applied Cognitive Psychology: The Official Journal of the Society for Applied Research in Memory and Cognition*, 23(8):1105–1121, 2009.

[43] Cuong V. Nguyen, Yingzhen Li, Thang D. Bui, and Richard E. Turner. Variational continual learning. In *International Conference on Learning Representations*, 2018. URL https://openreview.net/forum?id=BkQqq0gRb.

[44] Pingbo Pan, Siddharth Swaroop, Alexander Immer, Runa Eschenhagen, Richard Turner, and Mohammad Emtiyaz E Khan. Continual deep learning by functional regularisation of memorable past. *Advances in Neural Information Processing Systems*, 33:4453–4464, 2020.

[45] Anastasia Pentina and Christoph H Lampert. Lifelong learning with non-iid tasks. *Advances in Neural Information Processing Systems*, 28:1540–1548, 2015.

[46] Vinay V Ramasesh, Ethan Dyer, and Maithra Raghu. Anatomy of catastrophic forgetting: Hidden representations and task semantics. *arXiv preprint arXiv:2007.07400*, 2020.

[47] Sylvestre-Alvise Rebuffi, Alexander Kolesnikov, Georg Sperl, and Christoph H Lampert. icarl: Incremental classifier and representation learning. In *Proceedings of the IEEE conference on Computer Vision and Pattern Recognition*, pages 2001–2010, 2017.

[48] Matthew Riemer, Ignacio Cases, Robert Ajemian, Miao Liu, Irina Rish, Yuhai Tu, , and Gerald Tesauro. Learning to learn without forgetting by maximizing transfer and minimizing interference. In *International Conference on Learning Representations*, 2019. URL https://openreview.net/forum?id=B1gTShAct7.

[49] Anthony Robins. Catastrophic forgetting, rehearsal and pseudorehearsal. *Connection Science*, 7 (2):123–146, 1995.

[50] David Rolnick, Arun Ahuja, Jonathan Schwarz, Timothy Lillicrap, and Gregory Wayne. Experience replay for continual learning. *Advances in Neural Information Processing Systems*, 32, 2019.

[51] Mohammad Rostami, Soheil Kolouri, and Praveen K Pilly. Complementary learning for overcoming catastrophic forgetting using experience replay. *arXiv preprint arXiv:1903.04566*, 2019.

[52] Jonathan Schwarz, Wojciech Czarnecki, Jelena Luketina, Agnieszka Grabska-Barwinska, Yee Whye Teh, Razvan Pascanu, and Raia Hadsell. Progress & compress: A scalable framework for continual learning. In *International Conference on Machine Learning*, pages 4528–4537. PMLR, 2018.

[53] Joan Serra, Didac Suris, Marius Miron, and Alexandros Karatzoglou. Overcoming catastrophic forgetting with hard attention to the task. In *International Conference on Machine Learning*, pages 4548–4557. PMLR, 2018.

[54] Lloyd S Shapley. A value for n-person games, contributions to the theory of games, 2, 307–317, 1953.

[55] Dongsub Shim, Zheda Mai, Jihwan Jeong, Scott Sanner, Hyunwoo Kim, and Jongseong Jang. Online class-incremental continual learning with adversarial shapley value. In *Proceedings of the AAAI Conference on Artificial Intelligence*, volume 35, pages 9630–9638, 2021.

[56] Hanul Shin, Jung Kwon Lee, Jaehong Kim, and Jiwon Kim. Continual learning with deep generative replay. *arXiv preprint arXiv:1705.08690*, 2017.

[57] Gowthami Somepalli, Liam Fowl, Arpit Bansal, Ping Yeh-Chiang, Yehuda Dar, Richard Baraniuk, Micah Goldblum, and Tom Goldstein. Can neural nets learn the same model twice? investigating reproducibility and double descent from the decision boundary perspective. *arXiv preprint arXiv:2203.08124*, 2022.

[58] Sunil Thulasidasan, Gopinath Chennupati, Jeff A Bilmes, Tanmoy Bhattacharya, and Sarah Michalak. On mixup training: Improved calibration and predictive uncertainty for deep neural networks. *Advances in Neural Information Processing Systems*, 32, 2019.

[59] Michalis K. Titsias, Jonathan Schwarz, Alexander G. de G. Matthews, Razvan Pascanu, and Yee Whye Teh. Functional regularisation for continual learning with gaussian processes. In *International Conference on Learning Representations*, 2020. URL https://openreview.net/forum?id=HkxCzeHFDB.

[60] Gido M Van de Ven and Andreas S Tolias. Generative replay with feedback connections as a general strategy for continual learning. *arXiv preprint arXiv:1809.10635*, 2018.

[61] Gido M Van de Ven and Andreas S Tolias. Three scenarios for continual learning. *arXiv preprint arXiv:1904.07734*, 2019.

[62] Jeffrey S Vitter. Random sampling with a reservoir. *ACM Transactions on Mathematical Software (TOMS)*, 11(1):37–57, 1985.

[63] Liyuan Wang, Xingxing Zhang, Kuo Yang, Longhui Yu, Chongxuan Li, Lanqing HONG, Shifeng Zhang, Zhenguo Li, Yi Zhong, and Jun Zhu. Memory replay with data compression for continual learning. In *International Conference on Learning Representations*, 2022. URL https://openreview.net/forum?id=a7H7OucbWaU.

[64] Jaehong Yoon, Eunho Yang, Jeongtae Lee, and Sung Ju Hwang. Lifelong learning with dynamically expandable networks. *arXiv preprint arXiv:1708.01547*, 2017.

[65] Jaehong Yoon, Divyam Madaan, Eunho Yang, and Sung Ju Hwang. Online coreset selection for rehearsal-based continual learning. In *International Conference on Learning Representations*, 2022. URL https://openreview.net/forum?id=f9D-5WNG4Nv.

[66] Friedemann Zenke, Ben Poole, and Surya Ganguli. Continual learning through synaptic intelligence. In *International Conference on Machine Learning*, pages 3987–3995. PMLR, 2017.

[67] Hongyi Zhang, Moustapha Cisse, Yann N Dauphin, and David Lopez-Paz. mixup: Beyond empirical risk minimization. *arXiv preprint arXiv:1710.09412*, 2017.

[68] Linjun Zhang, Zhun Deng, Kenji Kawaguchi, Amirata Ghorbani, and James Zou. How does mixup help with robustness and generalization? In *International Conference on Learning Representations*, 2021. URL https://openreview.net/forum?id=8yKEo06dKNo.

[69] Amy Zhao, Guha Balakrishnan, Fredo Durand, John V Guttag, and Adrian V Dalca. Data augmentation using learned transformations for one-shot medical image segmentation. In *Proceedings of the IEEE/CVF conference on computer vision and pattern recognition*, pages 8543–8553, 2019.

[70] Yu Zheng, Zhi Zhang, Shen Yan, and Mi Zhang. Deep autoaugment. *arXiv preprint arXiv:2203.06172*, 2022.

Checklist

1. For all authors...
   1.1. Do the main claims made in the abstract and introduction accurately reflect the paper's contributions and scope? [Yes]
   1.2. Did you describe the limitations of your work? [Yes] See section G.
   1.3. Did you discuss any potential negative societal impacts of your work? [Yes] See section G.
   1.4. Have you read the ethics review guidelines and ensured that your paper conforms to them? [Yes]
2. If you are including theoretical results...
   2.1. Did you state the full set of assumptions of all theoretical results? [N/A]
   2.2. Did you include complete proofs of all theoretical results? [N/A]
3. If you ran experiments...
   3.1. Did you include the code, data, and instructions needed to reproduce the main experimental results (either in the supplemental material or as a URL)? [Yes]
   3.2. Did you specify all the training details (e.g., data splits, hyperparameters, how they were chosen)? [Yes] See section 4, F.
   3.3. Did you report error bars (e.g., with respect to the random seed after running experiments multiple times)? [Yes] See section 4.
   3.4. Did you include the total amount of compute and the type of resources used (e.g., type of GPUs, internal cluster, or cloud provider)? [Yes] See section F.
4. If you are using existing assets (e.g., code, data, models) or curating/releasing new assets...
   4.1. If your work uses existing assets, did you cite the creators? [Yes]
   4.2. Did you mention the license of the assets? [Yes]

4.3. Did you include any new assets either in the supplemental material or as a URL? [Yes]

4.4. Did you discuss whether and how consent was obtained from people whose data you're using/curating? [N/A]

4.5. Did you discuss whether the data you are using/curating contains personally identifiable information or offensive content? [N/A]

5. If you used crowdsourcing or conducted research with human subjects...

5.1. Did you include the full text of instructions given to participants and screenshots, if applicable? [N/A]

5.2. Did you describe any potential participant risks, with links to Institutional Review Board (IRB) approvals, if applicable? [N/A]

5.3. Did you include the estimated hourly wage paid to participants and the total amount spent on participant compensation? [N/A]

A Details of RAR based algorithms

Standard ER In Algorithm 2, we present the standard experience replay method [10, 49].

Algorithm 2 ER - Experience Replay based Continual Learning

Input: Tasks $(\mathcal{D}_1, \mathcal{D}_2, \ldots \mathcal{D}_T)$, Model θ, Learning Rate η, Memory $\mathcal{M}$, Memory Size m, Replay Budget k
Output: Model θ
for task $i \in [T]$ **do**
  for $(X_i, Y_i) \sim \mathcal{D}_i$ **do**
    $(X'_M, Y'_M) \sim \mathcal{M}$ { // randomly select k samples from memory}
    $\ell_{ER} \leftarrow \ell(X_i, Y_i; \theta) + \ell(X'_M, Y'_M; \theta)$
    $\theta \leftarrow \text{SGD}(\ell_{ER}, \theta, \eta)$
    $\mathcal{M} \leftarrow \text{ReservoirUpdate}(X_i, Y_i, \mathcal{M}, m)$
  end for
end for

ER-RAR In the ER-RAR method, we simply modify the replay sample selection step (line 6) of Alg. 1. As shown in line 6 of Algorithm 3, we rely on random sampling to get a subset of the buffer for replay.

Algorithm 3 ER-RAR - Retrospective Adversarial Replay for Continual Learning using vanilla ER as memory-retrieval method

1: **Input:** Tasks $(\mathcal{D}_1, \mathcal{D}_2, \ldots \mathcal{D}_T)$, Model θ, Learning Rate η, Memory $\mathcal{M}$, Memory Size m, Replay Budget k, Trade-off Parameter β, Perturbation Strength ϵ & number of gradient steps n
2: **Output:** Model θ
3: **for** task $i \in [T]$ **do**
4: **for** $(X_i, Y_i) \sim \mathcal{D}_i$ **do**
5: $\theta^{'} \leftarrow \text{SGD}(\ell(X_i, Y_i; \theta), \theta, \eta)$ { // Look-ahead update of model parameters}
6: $(X'_M, Y'_M) \sim \mathcal{M}$ { // randomly select k samples from memory}
7: Let $S := \emptyset$
8: **for** $x'_M \in X'_M$ **do**
9: $x'_i \in \text{argmin}_{x_i \in X_i, y(x'_M) \neq y(x_i)} \, d_{\theta'_l}(x'_M, x_i)$.
10: $S \leftarrow S \cup \{(x'_M, x'_i)\}$.
11: **end for**
12: $\ell_{RAR}(S, \theta, \theta') \leftarrow \sum_{(x'_M, x_i) \in S} \ell(g_{\theta'_l}(x'_M, x_i), y(x'_M); \theta)$ { // perform the targeted adversarial perturbations (Appendix H) and define the corresponding loss}
13: $\ell_{all} \leftarrow \ell(X_i, Y_i; \theta) + \beta \, \ell_{RAR}(S, \theta, \theta') + (1 - \beta) \, \ell(X'_M, Y'_M; \theta)$
14: $\theta \leftarrow \text{SGD}(\ell_{all}, \theta, \eta)$
15: $\mathcal{M} \leftarrow \text{ReservoirUpdate}(X_i, Y_i, \mathcal{M}, m)$
16: **end for**
17: **end for**

Discussion of MIR score and its intuition (find the buffered data suffering from the most amount of forgetting) The idea of probing to the next-step parameters θ' that we perform in RAR is similar to the Maximally Interfered Retrieval (MIR) method for memory/buffer retrieval [2], where we compute forgetting scores on the memory samples to identify a subset of memory samples that are negatively impacted by the current-task samples. The forgetting score of MIR for every sample in the memory buffer x_M is defined as follows:

$$\text{MIR}(x_M, \theta, \theta') := \ell(x_M, y(x_M); \theta') - \ell(x_M, y(x_M); \theta) \tag{8}$$

Then a subset of memory samples with the largest MIR scores i.e. having the greatest loss increase from θ to θ' are selected. We will denote such a subset as X'_M, i.e.

$$X'_M \in \underset{X \subseteq X_M, |X| \leq k}{\text{argmax}} \sum_{x \in X} \text{MIR}(x, \theta, \theta'). \tag{9}$$

Algorithm 4 MIR-RAR - Retrospective Adversarial Replay for Continual Learning using MIR as memory-retrieval method

Input: Tasks $(\mathcal{D}_1, \mathcal{D}_2, \ldots \mathcal{D}_T)$, Model θ, Learning Rate η, Memory $\mathcal{M}$, Memory Size m, Replay Budget k, Subset Size c, Trade-off Parameter β, Perturbation Strength ϵ & number of gradient steps n
Output: Model θ
for task $i \in [T]$ **do**
  for $(X_i, Y_i) \sim \mathcal{D}_i$ **do**
    $\theta^{'} \leftarrow \text{SGD}(\ell(X_i, Y_i; \theta), \theta, \eta)$ { // Look-ahead update of model parameters}
    $(X_M, Y_M) \sim \mathcal{M}$ { // randomly select c samples from memory}
    Compute $\text{MIR}(x_M, \theta, \theta')$ for $x_M \in X_M$ and select the subset X'_M based on Eq. 9 s.t. $|X'_M| = k$
    Let $S := \emptyset$.
    for $x'_M \in X'_M$ **do**
      $x'_i \in \text{argmin}_{x_i \in X_i, y(x'_M) \neq y(x_i)} \, d_{\theta'_l}(x'_M, x_i)$.
      $S \leftarrow S \cup \{(x'_M, x'_i)\}$.
    end for
    $\ell_{RAR}(S, \theta, \theta') \leftarrow \sum_{(x'_M, x_i) \in S} \ell(g_{\theta'_l}(x'_M, x_i), y(x'_M); \theta)$ { // perform the targeted adversarial perturbations (Appendix H) and define the corresponding loss}
    $\ell_{all} \leftarrow \ell(X_i, Y_i; \theta) + \beta \, \ell_{RAR}(S, \theta, \theta') + (1 - \beta) \, \ell(X'_M, Y'_M; \theta)$
    $\theta \leftarrow \text{SGD}(\ell_{all}, \theta, \eta)$
    $\mathcal{M} \leftarrow \text{ReservoirUpdate}(X_i, Y_i, \mathcal{M}, m)$
  end for
end for

Intuitively, X'_M contains samples that are most confusing with the incoming ones, and thus using such samples as the anchor samples would result in more successful adversarial perturbations.

As we need to compute θ' for the retrospective adversarial samples, the MIR score does not incur extra computations. Moreover, we can also utilize the subset X'_M as additional training signals similar to the MIR approach, which allows us to trade-off between the adversarially perturbed data points versus real data points that are uniformly sampled from previous tasks.

Algorithm 5 mix-RAR - Retrospective Adversarial Replay for Continual Learning using MixUp

Input: Tasks $(\mathcal{D}_1, \mathcal{D}_2, \ldots \mathcal{D}_T)$, Model θ, Learning Rate η, Memory $\mathcal{M}$, Memory Size m, Replay Budget k, Subset Size c, Trade-off Parameter β, Perturbation Strength ϵ & number of gradient steps n
Output: Model θ
for task $i \in [T]$ **do**
  for $(X_i, Y_i) \sim \mathcal{D}_i$ **do**
    $\theta^{'} \leftarrow \text{SGD}(\ell(X_i, Y_i; \theta), \theta, \eta)$ { // Look-ahead update of model parameters}
    Select (X'_M, Y'_M) from $\mathcal{M}$ s.t. $|X'_M| = k$ { // using existing memory-retrieval methods}
    $\tilde{X}'_M, \tilde{Y}'_M = \text{mixup}(X'_M, Y'_M, \alpha)$ { // perform mixup on replay samples}
    Let $S := \emptyset$
    for $\tilde{x}_M \in \tilde{X}'_M$ **do**
      $x'_i \in \text{argmin}_{x_i \in X_i, y(\tilde{x}_M) \neq y(x_i)} \, d_{\theta'_l}(\tilde{x}_M, x_i)$.
      $S \leftarrow S \cup \{(\tilde{x}_M, x'_i)\}$.
    end for
    $\ell_{RAR}(S, \theta, \theta') \leftarrow \sum_{(\tilde{x}_M, x_i) \in S} \ell(g_{\theta'_l}(\tilde{x}_M, x_i), y(\tilde{x}_M); \theta)$ { // perform the adversarial perturbations (Appendix H) and define the corresponding loss}
    $\ell_{all} \leftarrow \ell(X_i, Y_i; \theta) + \beta \, \ell_{RAR}(S, \theta, \theta') + (1 - \beta) \, \ell(X'_M, Y'_M; \theta)$
    $\theta \leftarrow \text{SGD}(\ell_{all}, \theta, \eta)$
    $\mathcal{M} \leftarrow \text{ReservoirUpdate}(X_i, Y_i, \mathcal{M}, m)$
  end for
end for

MIR-RAR In Algorithm 4, we change line 6 of Algorithm 1 to use the MIR score to select the replay subset X'_M.

mix-RAR In the mix-RAR method detailed in Algorithm 5, after selecting the replay samples X'_M (using ER, MIR, ASER, etc.) from the memory $\mathcal{M}$, we simply apply MixUp [67] to perform perturbations/editing on the replay examples. Mixup generates virtual training samples $\tilde{x}_M, \tilde{y}_M$ by taking convex combinations of pairs of inputs and their labels.

$$\tilde{x}_M = \lambda x_i + (1-\lambda) x_j \qquad \tilde{y}_M = \lambda y_i + (1-\lambda) y_j \tag{10}$$

where $x_i, x_j \in X'_M$ and $y_i, y_j \in Y'_M$ and $\lambda \in [0, 1]$ is drawn from a Beta distribution $\lambda \sim \text{Beta}(\alpha, \alpha)$, where α is a hyperparameter.

We, then pair up these virtual samples with the current's task samples based on the distance function defined in Eq. 5 and use Eq. 4 to perturb them such that in the representation space modeled by θ'_l, the augmentation of the virtual samples are closer to the paired sample from the current task, than the source/anchor samples x_i and x_j.

B Details of Related Work

We include detailed explanations about prior works which are relevant in the context of task-free continual learning:

- **Experience Replay (ER)** [10, 49]: ER maintains previously seen examples in a limited size constrained memory buffer for future replay. It deals with the problem of memory retrieval and can be used in both task-free as well as task-dependent continual learning settings, but in all experiments in this paper, we use it as a task-free CL method. As a new incoming batch from current task comes in, we draw a subset of examples from the buffer such that the size of the drawn subset is same as the incoming batch size. In all experiments, we fix this subset size (also referred to as the replay budget) as 10.
- **Gradient Episodic Memory (GEM)** [37]: GEM also maintains an episodic memory for each observed task. As a new incoming batch comes in, GEM projects the gradient of the model parameters such that loss incurred on the episodic memory maintained for each task does not increase while learning a new task. This approach, thus needs access to the task-ids, and is computationally intensive owing to solving a QP program at each iteration of training.
- **Averaged Gradient Episodic Memory (A-GEM)** [9]: Averaged-GEM is an improvement over GEM in terms of relaxing the need to require task-ids. In stead of constraining the model parameters using the entire stored buffer, it randomly samples a subset of examples from the memory buffer to regularize the model parameters in order to minimize forgetting on previously seen tasks.
- **Gradient-based Sample Selection (GSS)** [3]: GSS deals with the problem of Memory Update in task-free CL setting. It aims to maximize samples diversity in the gradient space while selecting examples for memory update. The performance improvement observed is significant when different tasks data are imbalanced. In all experiments covered in this paper, we have used reservoir sampling as the memory update method over all compared SoTA methods to ensure fair comparison.
- **Maximally Interfered Retrieval (MIR)** [2]: MIR is another memory retrieval method which does not need access to task-ids while selecting buffer exemplars for replay. It proposes to first perform a virtual update (one-step look-ahead update) only on the incoming batch of the current batch. It then computes the interference on the memory samples in terms of the loss increase observed w.r.t. the virtual updated model parameters, and selects those buffer samples for which the loss increase is maximum — it selects the maximum interfered/forgotten samples from the buffer. The implementation code provided by the authors that we have used is located at https://github.com/optimass/Maximally_Interfered_Retrieval.
- **Adversarial Continual Learning (ACL)** [16]: ACL focuses on learning two kind of features for task-dependent CL: (1) shared task-invariant (2) task specific features. The architecture grows as a new task comes by adding a task-specific module. It utilizes adversarial learning to train a shared feature encoder and a discriminator using the classic

minimax optimization objective (as used by GANs). The role of the discriminator is to correctly classify the encoded features by their task labels/ids while the role of the encoder is to generate task-invariant features that can fool the discriminator. RAR, on the other hand, focuses on the static architecture task-free CL and utilizes the idea of adversarial perturbations in the input space to perturb the memory replay samples such that they are located close to the forgetting frontier w.r.t. to the current tasks.

- **Adversarial Shapley Value Experience Replay (ASER)** [55]: ASER proposes a scoring method based on kNN Shapley Value (SV) to select memory samples which are representative of the stored memory samples and adversarially close to the decision boundaries of new classes. On the other hand, RAR's objective is to minimize the worst-case experience replay loss by generating targeted adversarial replay perturbations that are visually similar to the chosen replay samples but the CL model mistakes them for the nearest class (from the incoming batch) based on their distance from the decision boundaries. When we apply RAR's objective on ASER chosen replay samples (i.e., compute X'_M in Sec 3.2 using Adversarial SV), both accuracy and forgetting improve quite significantly (Table 1, 2), suggesting that learning on the RAR's adversarial perturbations helps the model to learn about the boundaries between past and current tasks. Also, we use Adversarial SV only for memory retrieval in order to ensure fair comparison across all methods. The implementation code provided by the authors is at https://github.com/RaptorMai/online-continual-learning.

- **Gradient-based Memory Editing for Continual Learning (GMED)** [25]: GMED uses gradient updates to edit/perturb the stored replay samples, to create more challenging samples for rehearsal in a task-free setting. This work is most relevant to RAR. While their objective aims to perturb samples individually to generate increased losses in the upcoming model updates, our method looks into the local pairwise relationships between the most interfered memory samples and the new task's samples. By utilizing such information, we locally perturb each replay sample in a targeted adversarial manner. The model then confuses them with the new tasks' data, creating more confusing examples close to the forgetting frontier as well as representative of previous data. The implementation code provided by the authors is at https://github.com/INK-USC/GMED.

C Reservoir Sampling

Algorithm 6 Reservoir Update

Input: Samples (x_t, y_t), Buffer $\mathcal{M}$, reservoir/buffer size m
if $|\mathcal{M}| < m$ **then**
  $\mathcal{M} = \mathcal{M} \cup (x_t, y_t)$
else
  $j = \text{randint}(1, t)$
  if $j \leq m$ **then**
    $\mathcal{M}[j] \leftarrow (x_t, y_t)$
  end if
end if

We use traditional reservoir sampling method [62] detailed in Alg. 6 to update the limited memory buffer when a new batch's data comes in. Reservoir sampling uniformly samples from the incoming task's stream by assigning a sampling probability of m/t where t is the number of samples seen so far. It does not need any prior information about the length of the complete data stream.

Prior works based on task-free continual learning [2, 33, 37] have shown promising results when using reservoir sampling as the memory update method. [26, 37] have proposed modified versions of reservoir sampling which help populate the memory with diverse samples in a balanced way when dealing with heterogeneous and long-tailed data streams. Since, in this work, our focus is primarily on class-balanced datasets, we use Reservoir Sampling as the memory update method and plan to study other memory update methods which can be balanced in terms of the present classes in future work.

Table 4: Class-incremental Continual Learning Datasets Statistics

	Split-MNIST	Split-CIFAR10	Split-CIFAR100	Split-miniImageNet
# of tasks	5	5	20	20
# of classes per task	2	2	5	5
# of training samples per task	1000	10000	2500	2500
# of test samples per task	2000	2000	500	500
# of overall classes	10	10	100	100

D Dataset Details

Based on the taxonomy described in [61], the datasets that we studied fall under the *class-incremental* (CI) category. The dataset details are as follows:

Split-MNIST is a variant of the MNIST dataset (http://yann.lecun.com/exdb/mnist/) of handwritten digits [31] split into five disjoints tasks based on the labels. Each task consists of two classes, and we use only 1k examples from each task for training and report results on the complete test set. The goal is to classify all ten classes at the end of the last task.

Split-CIFAR10 is a variant of the CIFAR-10 dataset [28] (https://www.cs.toronto.edu/ kriz/cifar.html) split into 5 disjoint tasks based on labels. Each task consists of two classes and 10k training examples.

Split-CIFAR100 is a variant of the CIFAR-100 dataset (https://www.cs.toronto.edu/ kriz/cifar.html) comprises of 20 disjoint tasks with each task dealing with 5 classes. This is 100-way classification problem since we do not use any task information during training/testing.

Split-miniImageNet splits the mini-ImageNet dataset [14] (https://lyy.mpi-inf.mpg.de/mtl/download/) into 20 disjoint tasks based on labels. Each task comprises of 5 classes and 2.5k training examples.

In Table 4, we present the statistics of all four datasets. Training samples used for each task is 95% of the mentioned numbers as 5% is held-out as validation set. For fine-tuning the hyper-parameters associated with the RAR framework, we use the held-out validation set. In case of Split-MNIST dataset, following the setting of previous methods such as [2, 25], we use only 1000 training examples per task.

E Complexity Analysis

We compare the replay-based methods in terms of forward and backward computations used, besides the forward features computed on the incoming batch X_i and backward pass used for the final parameters updates:

1. **ER**: 1 extra forward pass on the replay samples i.e. $f(X'_M; \theta)$
2. **ER-RAR**: 1 backward pass for the virtual model update to θ', n forward and backward passes to generate the targeted augmentations of X'_M using θ' where n denotes the number of iterative steps used to generate the RAR data, 1 forward pass on the replay examples and the generated RAR data using θ.
3. **MIR**: 1 backward pass for the virtual model update to θ', 2 forward passes on the larger memory set, i.e. $f(X_M; \theta)$, $f(X_M; \theta')$, 1 forward pass on the smaller set of replay samples i.e., $f(X'_M; \theta)$.
4. **MIR-RAR**: 1 backward pass for the virtual model update to θ', 2 forward passes on the larger memory set, i.e. $f(X_M; \theta)$, $f(X_M; \theta')$, n forward and backward passes to generate the targeted augmentations of X'_M using θ' where n denotes the number of iterative steps used to generate the RAR data, 1 forward pass on the smaller set of original replay samples and the RAR augmented data using θ.

Thus, comparing ER-RAR w.r.t ER, ER-RAR needs n extra forwards passes and $(n + 1)$ extra backward passes on top of ER. Similarly, MIR-RAR adds n additional forward and backwards passes on top of MIR. Setting $n = 2$ for all datasets (except Split-MNIST with 1000 training samples per

task) meaning using only two gradient steps to optimize the RAR augmentation objective defined in Eq. 4 in the input space, we limit the additional computational costs introduced by RAR.

Computational costs reduction based on Sec 3.2 and 3.3: Instead of using all $|X_M|$ examples in the memory buffer $\mathcal{M}$, replay data selection reduces the potential candidates to be considered for adversarial data generation to $|X'_M|$. For example, given a buffer size of 500 and replay budget of $k = 10$, the potential buffer samples considered for generating RAR adversarial augmentations is only 10 instead of 500.

Having reduced the size of the replay set to $|X'_M|$, one would still need to consider every potential pairing between X'_M and X_i (current task samples) to find the most confusing subset of cardinality c which incurs maximum RAR loss defined in Eq. 3. Here, c is essentially the replay budget. Generating targeted adversarial samples for each pair can be computationally prohibitive. Our nearest neighbor-based pairing brings down the number of adversarial samples to be generated (by optimizing Eq. 3) to c from $|X'_M| \times |X_i|$. In the above example for a current batch size of 10, we only need to generate $c = 10$ targeted adversarial samples to approximately optimize Eq. 3 instead of generating 10×10 adversarial samples and then choosing c samples with the largest RAR loss.

F Implementation Details

Following the current SoTA methods [2, 10, 25], we use a MLP classifier with two hidden layers as the backbone architecture for Split-MNIST dataset. For remaining datasets, we use the reduced ResNet-18 classifier [22] with the output layer having as many units as the number of classes present in the entire dataset. In all experiments based on experience replay methods, we use SGD optimizer with a learning rate of 0.1 for all datasets. For GMED [25], ASER [55] based methods, we present the results using the set of hyperparameters reported in the papers. Both mini-batch size and replay budget are set to 10 following above mentioned methods to make the comparisons fair. For MIR based methods, we set the subset size c to 50 for all datasets following [2]. c denotes the size of the larger set of buffer examples on which the forgetting/interference score is computed.

Hyperparameters Tuning: We tune the hyperparameters associated with the RAR framework $\{n, \beta, \epsilon\}$ on the held-out validation set across all datasets. For all datasets, we analyze (as shown in Figure 5) the sensitivity of the performance of RAR in terms of the number of gradient steps n used to perform the constrained targeted optimization in the input space as shown in Eq. 4. Specifically, we study values of $n \in \{2, 5, 10\}$. Based on the trade-off between the performance and the computational costs associated with the forward and backward passes employed to generate the targeted adversarial augmentation, we set $n = 2$ for all datasets except for Split-MNIST where we set $n = 5$ based on the average forgetting score as shown in Fig. 5a. Since the MNIST dataset is relatively easier to train on, more gradient steps are needed to generate difficult samples which are indiscernible for the model in the learnt representation space after the look-ahead update on the new task's data.

For the weight assigned to the ℓ_{RAR} computed using Eq. 3 in the final loss objective (denoted by β), we search over $\{0.05, 0.075, 0.1, 0.2, 0.3, 0.4, 0.5\}$ and fine-tune them separately for different datasets across various buffer sizes that we study. For Split-MNIST, β equal to $0.3, 0.3$, and 0.4 lead to the best reported performance across buffer size $200, 500$, and 1000 respectively. For Split-CIFAR10, these values are $0.5, 0.1$, and 0.075 for buffer sizes $200, 500$, and 1000 respectively. For Split-CIFAR100 and Split-miniImageNet, we get the best setting as $\beta = 0.4$.

We search for the best perturbation tolerance ϵ hyperparameter in $\{0.15, 0.3\}$ for Split-MNIST, $\{0.0314, 0.07\}$ for Split-CIFAR10 and Split-CIFAR100, and $\{0.01568, 0.0314\}$ for Split-miniImageNet. The best setting ϵ values are 0.3 for Split-MNIST and 0.0314 for remaining three datasets.

Prior works such as [46] show that the deeper/higher layers of neural networks are disproportionately responsible for catastrophic forgetting in line with the observation that the shallower/lower layers learn general features of and higher layers learn more task-specific features. Therefore, we use the penultimate layer (layer just before the final classification/softmax layer) as layer l in Eq. 4 and in the representation space of θ'_l, we minimize the augmentation objective such that the penultimate feature embedding of the RAR augmented sample and its paired current task sample are as close as possible, but visually still similar to the original buffer sample.

Compute Resources: We use a single NVIDIA GeForce GTX 1080 Ti to train our CL models. The PyTorch and CUDA toolkit versions used are 1.6.0 and 10.1 respectively.

G Limitations & Societal Impacts

Limitations: In this work, we have utilized Reservoir Sampling across all compared methods to update the memory/buffer as a new batch comes in. Using other recently proposed methods [3, 55] to tackle this problem could potentially help in maintaining a diverse & representative memory/buffer, particularly in case of class-imbalanced incremental datasets. We also plan to explore updating the memory/buffer with perturbed samples (in stead of original samples) and see if re-learning them at later stages of training could help ameliorate forgetting. Similar to other CL algorithms, our work is validated on small datasets with single pass training on streams generated in a synthetic fashion. Therefore, the final average accuracy achieved on all set of classes is significantly small compared to traditional (i.i.d. assumption based) supervised training on the entire dataset.

Negative Societal Impacts: The potential improvements brought in terms of mitigating forgetting while learning on a continual stream of data might have some indirect negative impact. For example, as spam detection systems are updated to prevent spam, bots can learn to continually evolve to defeat them. Similar issues could arise in other surveillance systems in place. The replay of RAR augmentations might introduce some bias if malicious attackers can manipulate the data stream in the continual learning setting.

H Background on Targeted Adversarial Augmentations (or Attacks) & Related Algorithms

Given a model θ, associated layer l of the model, source input-output pair (x_s, y_s) and a target input-output pair (x_t, y_t), the goal of targeted adversarial attack/perturbation is to generate an input z which looks visually similar to the source input x_s, but in the latent space of model's l-th layer, the feature embedding of z is close to the feature embedding of the target input x_t.

The objective can be mathematically summarized as:

$$g_{\theta_l}(x_s, x_t) \in \underset{z}{\operatorname{argmin}}\, \mathcal{L}_{\theta_l}(z, x_t) \tag{11}$$

$$\text{s.t. } ||z - x_s||_\infty \leq \epsilon \tag{12}$$

Here, if we use the model's last layer denoted by L, then often times $\mathcal{L}_{\theta_l}(z, x_t)$ can be replaced with the cross-entropy loss w.r.t. to the target label y_t of the paired sample x_t i.e., $\ell(z, y_t; \theta)$.

In case we use layer l such that $l < L$, meaning layers lower/shallower than the last layer, one can use the defined distance function in Eq. 5 i.e., $d_{\theta_l}(z, x_t) := ||\theta_l(z) - \theta_l(x_t)||_2$ as the minimization objective $\mathcal{L}_{\theta_l}(z, x_t)$ in the above constrained optimization problem.

The Fast Gradient Sign Method (FGSM) proposed in [20] can be used to solve Eq. 11 when dealing with infinity norm constraints in the input space. Specifically:

$$g_{\theta_l}(x_s, x_t) = x_s - \epsilon \cdot \text{sign}(\nabla_{x_s} \mathcal{L}_{\theta_l}(x_s, x_t)) \tag{13}$$

where $\nabla_{x_s} \mathcal{L}_{\theta_l}(x_s, x_t)$ is the gradient of the loss function in Eq. 11 w.r.t. x_s.

Iterative-FGSM [30] which iteratively applies FGSM n times with a smaller step size α (proportional to ϵ/n) can also be used. Here n denotes the number of iterations used to iteratively optimize Eq. 11.

To stabilize the gradient update directions and avoid poor local maxima, [15] proposed Momentum-Iterative FGSM (MI-FGSM) which integrates momentum with a decay factor μ and accumulates the gradients of previous iterations while updating the targeted augmentation at each step.

At step $t = 0$, we initialize $x_s^0 = x_s$. Then, at step t, the accumulated gradient and targeted augmentation are derived as follows (the superscript t denotes the iteration step, while the subscript t denotes the target example):

$$g^{t+1} = \mu \cdot g^t + \frac{\nabla_{x_s} \mathcal{L}_{\theta_l}(x_s^t, x_t)}{||\nabla_{x_s} \mathcal{L}_{\theta_l}(x_s^t, x_t)||_1} \tag{14}$$

$$x_s^{t+1} = x_s^t - \alpha \cdot \text{sign}(g^{t+1}) \tag{15}$$

At the end of each step, we project back into the norm ball $||x_s^{t+1} - x_s||_\infty \leq \epsilon$ and we also clip the values back to the input range observed corresponding to the original pixel values when using image data. In this work, we use MI-FGSM with the decay factor μ as 1.0, the step-size α same as ϵ since we employ only two iterations to generate the RAR augmented data using buffer replay samples (X'_M, Y'_M) as the source/anchor sample. The paired sample from the incoming batch of current task (X_i, Y_i) can be seen as the target sample.

I Additional Experiments

Table 5: Comparison of RAR with other non-RAR baselines having similar computational costs. Numbers within bracket denote the overall buffer size used.

	Split-MNIST (200)		Split-CIFAR10 (200)		Split-CIFAR10 (500)		Split-CIFAR10 (1000)	
Method	Accuracy (↑)	Forgetting (↓)	Accuracy	Forgetting	Accuracy	Forgetting	Accuracy	Forgetting
ER-3-iters	82.3 ± 0.8	17.6 ± 0.8	28.5 ± 1.3	52.5 ± 3.7	36.1 ± 1.5	39.5 ± 2.1	41.5 ± 1.2	30.8 ± 1.9
ER-GMED	82.5 ± 1.4	15.0 ± 1.7	30.4 ± 0.9	39.0 ± 1.3	38.3 ± 1.1	27.7 ± 1.3	42.8 ± 1.5	20.5 ± 1.2
ER-RAR (ours)	$\mathbf{84.0 \pm 1.1}$	$\mathbf{11.8 \pm 1.5}$	$\mathbf{33.2 \pm 1.4}$	$\mathbf{37.6 \pm 2.1}$	$\mathbf{40.4 \pm 1.7}$	$\mathbf{25.1 \pm 2.5}$	$\mathbf{44.0 \pm 1.4}$	$\mathbf{18.1 \pm 2.0}$
MIR-3-iters	83.1 ± 0.8	15.3 ± 1.4	28.4 ± 1.0	53.4 ± 2.1	41.1 ± 0.8	33.3 ± 1.5	$\mathbf{48.9 \pm 1.1}$	22.4 ± 1.9
MIR-GMED	84.2 ± 1.2	12.2 ± 1.0	27.5 ± 1.3	45.5 ± 1.6	37.2 ± 1.1	28.6 ± 1.9	43.0 ± 1.5	17.6 ± 2.1
MIR-RAR (ours)	$\mathbf{86.2 \pm 0.6}$	$\mathbf{9.1 \pm 0.8}$	$\mathbf{33.3 \pm 1.1}$	$\mathbf{33.5 \pm 2.2}$	$\mathbf{43.1 \pm 1.1}$	$\mathbf{21.1 \pm 2.2}$	45.3 ± 1.5	$\mathbf{14.1 \pm 1.6}$

To ensure fair comparison in terms of computational costs (extra forward and backward passes as described in Sec. E), in Table 5, we compare RAR to GMED [25], ER-3-iters, and MIR-3-iters. 3-iters means that the model is trained for three iterations on the incoming batch and buffer samples as a new batch comes in. GMED also performs multiple iterations of gradient updates to edit/perturb the buffer samples. Across all compared methods, RAR-based methods perform significantly better in terms of forgetting (lower is better) as well as final accuracy.

Comparison to knowledge distillation based methods: On Split-CIFAR10 dataset for two different buffer sizes, we augment RAR with DER [6] which utilizes knowledge distillation in the logits space. DER which imposes regularization in the logits space can be seen as a complimnetary method to RAR and we observe that combining them together leads to further improvements in Table 6. ER-DER is essentially DER that uses random sampling to select the replay samples and was proposed in the DER paper. In MIR-DER, we use MIR scores to select the replay batch for DER. In Table 6, *aug* means that we apply standard augmentations such as random cropping and rotations on the replay samples.

Table 6: Comparison of RAR with DER (with and without augmentation) to non-RAR baselines. Numbers within bracket denote the overall buffer size used.

	Split-CIFAR10 (200)		Split-CIFAR10 (500)	
Method	Accuracy (↑)	Forgetting (↓)	Accuracy (↑)	Forgetting (↓)
ER-DER	28.0 ± 1.3	47.2 ± 7.2	32.9 ± 1.9	28.4 ± 3.3
ER-RAR-DER	36.0 ± 1.6	21.2 ± 2.6	39.8 ± 0.5	15.5 ± 2.2
ER-DER-aug	34.0 ± 3.3	37.4 ± 7.6	39.6 ± 1.5	18.2 ± 4.1
ER-RAR-DER-aug	36.7 ± 1.5	15.8 ± 2.3	40.3 ± 1.1	10.3 ± 1.9
MIR-DER	36.6 ± 2.3	20.0 ± 1.5	38.6 ± 1.7	10.8 ± 1.9
MIR-RAR-DER	35.9 ± 1.9	20.1 ± 3.3	38.5 ± 0.8	10.8 ± 1.8
MIR-DER-aug	36.5 ± 2.3	17.0 ± 1.8	39.5 ± 1.0	15.0 ± 1.7
MIR-RAR-DER-aug	37.2 ± 1.8	13.4 ± 1.1	40.1 ± 0.8	9.5 ± 2.3

Comparison to other augmentation techniques: In Table 3, we compare RAR to another perturbation method *random* which adds random noise of the same perturbation magnitude as RAR, and show that RAR leads to significant improvement in reducing forgetting as well as increasing the average accuracy on different CL benchmark datasets. In Table 7, we compare to other standard augmentations techniques such as random cropping and rotations applied to the replay samples. Utilizing these standard augmentation strategies along with RAR leads to impressive improvements in terms of the forgetting metric as shown in Table 7.

When using standard augmentations along with RAR, ER-RAR-aug and MIR-RAR-aug achieve similar performance irrespective of the memory retrieval/selection method used. This indicates that RAR, when combined with standard augmentations such as random cropping and rotations, is more

Table 7: Comparison of RAR to standard augmentation techniques. Numbers within bracket denote the overall buffer size used.

	Split-CIFAR10 (200)		Split-CIFAR10 (500)	
Method	Accuracy (↑)	Forgetting (↓)	Accuracy (↑)	Forgetting (↓)
ER	25.7 ± 1.3	51.3 ± 4.1	31.9 ± 0.9	39.0 ± 2.1
ER-aug	30.0 ± 4.1	43.2 ± 6.9	39.4 ± 2.8	26.0 ± 6.3
ER-RAR	33.2 ± 1.4	37.6 ± 2.1	40.4 ± 1.7	25.1 ± 2.5
ER-RAR-aug	39.3 ± 1.6	21.6 ± 3.4	42.2 ± 1.9	13.6 ± 2.5
MIR	28.0 ± 1.5	48.1 ± 2.9	37.5 ± 1.6	32.2 ± 2.1
MIR-aug	36.1 ± 2.6	23.7 ± 3.6	40.5 ± 1.2	18.4 ± 3.3
MIR-RAR	33.3 ± 1.1	33.5 ± 2.2	43.1 ± 1.1	21.1 ± 2.2
MIR-RAR-aug	41.6 ± 1.2	21.0 ± 2.8	42.2 ± 2.3	12.5 ± 2.6

robust to replay data selection and can generate high-quality replay samples (diverse, confusing, and representative of previously seen tasks).

However, such augmentation strategies rely on strong human priors, and manually selecting such augmentation operators requires domain expertise and prior knowledge of the dataset of interest [70]. They may perform poorly in the scenarios when human knowledge is weak for the targeted domain. For example, for medical image analysis, such simple transformations are shown to be insufficient in capturing many of the subtle variations present in the data [69]. Moreover, they are static and pre-defined before the training so they cannot capture the training dynamics during the continual learning process for the purpose of reducing the forgetting. RAR, on the other hand, automatically generates augmentations adaptive to the forgetting dynamics of the model and thus focuses on reducing the local interference near the forgetting frontier between different tasks.

Virtual update for RAR samples generation: When training sequentially on a set of tasks, catastrophic forgetting of previous tasks occurs as the network weights become biased to meet the objectives of the new task. Performing a single-step virtual update of the model by exposing it only to the current task's data helps us explore which buffer samples are most likely to be forgotten. We use θ', the virtually updated model to generate the adversarial samples using Eq. 4 as such perturbed samples are likely to be forgotten in future updates and confused with the current task's classes leading to increased loss on them. In retrospect, using the generated perturbed sample (visually close to the original sample x_M in the input space and hence in-distribution) with its correct label $y(x_M)$ and replaying it while we are still at θ helps in alleviating forgetting. As we combine the losses, we may also consider the procedure as first doing an update on the incoming task to get θ' and then performing an adversarial training step based on θ' using the RAR augmented samples.

One can argue that the step size used to perform this virtual update (η_{virtual}) could be different from the step size (η) used to update the continual learner such that the adversarial samples generated using θ' are not too easy or too hard to classify by the current model θ. We perform experiments on the Split-CIFAR10 dataset with a buffer size of 500 and an SGD optimizer with a learning rate (η) of 0.1. We find that using the same learning rate as the SGD optimizer to perform the virtual update results in the best performance on MIR-RAR as shown in Table 8.

Table 8: Performance of MIR-RAR for different values of η_{virtual} when $\eta = 0.1$

η_{virtual}	Accuracy (↑)	Forgetting (↓)
No virtual update	41.7 ± 1.3	21.8 ± 1.4
0.02	42.1 ± 1.6	22.1 ± 2.8
0.05	42.6 ± 1.1	20.6 ± 3.7
0.1	43.1 ± 1.1	21.1 ± 2.2
0.15	43.1 ± 1.6	22.1 ± 3.5
0.2	41.9 ± 1.1	23.1 ± 3.6

Ratio between incoming mini-batch size and replay budget: Following prior works [2, 25, 55], we select the same number of replay samples from the buffer as the mini-batch size of the incoming new task. This is set to 10 irrespective of the buffer size. Here, we perform additional experiments where we vary the ratio between the incoming mini-batch size and replay budget. As expected, when

the combined batch is dominated primarily by the incoming task samples (mini-batch size / replay budget = 15/5), we observe a significant drop on the overall performance with respect to both the average accuracy and forgetting as shown in Table 9. However, when replaying more samples from the buffer (mini-batch size / replay budget = 5/15) in each training iteration, which over-compensates for forgetting, we do not observe any improvement in reducing the forgetting. This suggests that to achieve a good plasticity-stability trade-off, the ratio between incoming mini-batch size and replay budget need to be close to one.

Table 9: Performance of replay-based CL methods when using different ratios between incoming mini-batch size and replay budget. Dataset used is Split-CIFAR10 with a buffer size of 500.

Ratio	**10/10**		**5/15**		**15/5**	
Method	Accuracy (↑)	Forgetting (↓)	Accuracy (↑)	Forgetting (↓)	Accuracy (↑)	Forgetting (↓)
ER	31.9 ± 0.9	39.0 ± 2.1	30.5 ± 2.7	53.0 ± 4.4	20.9 ± 2.1	55.7 ± 6.1
ER-RAR	40.4 ± 1.7	25.1 ± 2.5	40.2 ± 2.2	26.0 ± 3.2	26.0 ± 3.6	31.4 ± 3.5
MIR	37.5 ± 1.6	32.2 ± 2.1	37.4 ± 1.4	35.1 ± 2.0	16.5 ± 1.5	68.5 ± 3.3
MIR-RAR	43.1 ± 1.1	21.1 ± 2.2	41.0 ± 1.4	22.9 ± 3.2	18.6 ± 2.6	58.0 ± 5.1

J Visualizations of Learnt Decision Regions

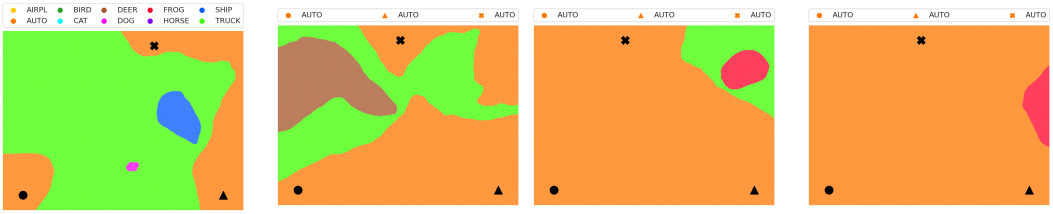

(a) ER (b) MIR (c) MIR-RAR (d) MIR-mix-RAR

Figure 7: Decision regions are generated using a triplet of training samples on which the model makes the right predictions. All samples are from same class *Auto (Task 1)*. Legend in (a) applies to all and describes the color used to denote different classes. Remaining legends denote the classes corresponding to the chosen triplet samples.

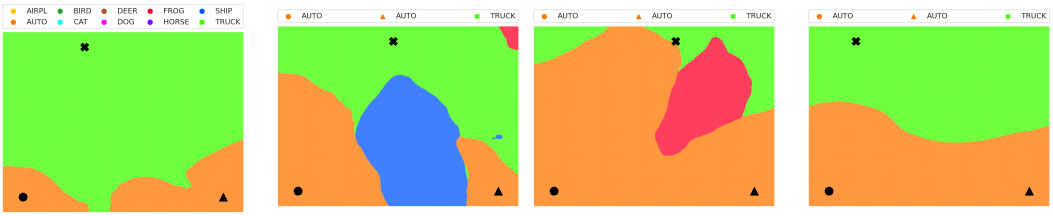

(a) ER (b) MIR (c) MIR-RAR (d) MIR-mix-RAR

Figure 8: Decision regions are generated using a triplet of training samples on which the model makes the right predictions. Two samples belong to class *Auto (Task 1)*, while the third samples is from class *Truck (Task 5)*. Legend in (a) applies to all and describes the color used to denote different classes. Remaining legends denote the classes corresponding to the chosen triplet samples.

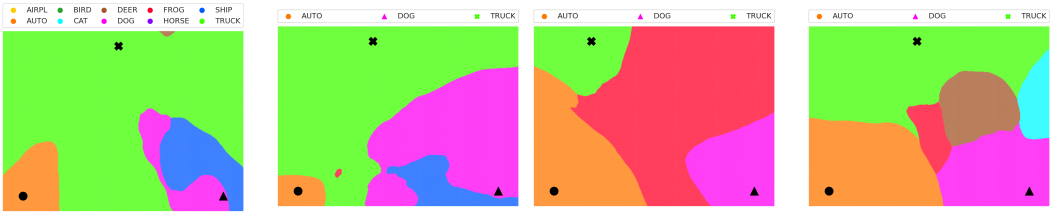

(a) ER (b) MIR (c) MIR-RAR (d) MIR-mix-RAR

Figure 9: Decision regions are generated using a triplet of training samples on which the model makes the right predictions. Samples are from the following classes: *Auto (Task 1), Dog (Task 3), Truck (Task 5)*. Legend in (a) applies to all and describes the color used to denote different classes. Remaining legends denote the classes corresponding to the chosen triplet samples.

Inspired from recent works in decision boundaries visualization [57], we try to visualize the decision regions learnt by the continual learner along the data manifold. To plot the decision regions, we use the plotting technique from [57] (https://github.com/somepago/dbViz). Using a sampled triplet of data points (x_1, x_2, x_3), we construct a plane spanned by vectors $\overrightarrow{v_1} = x_2 - x_1$ and $\overrightarrow{v_2} = x_3 - x_1$ and plot decision regions in this plane.

Specifically, for our use-case, once the training on all tasks (5 in case of Split-CIFAR10) is finished, we use the trained model to make predictions on the trained data. We, then, select three training set instances (x_1, x_2, x_3) on which the model makes the correct predictions in following ways: (1) all samples are from the same class, (2) two samples share the same class label while the third belongs to a different class, and (3) all three samples are from different classes.

We analyze the decision regions learnt by the ResNet-18 model using ER [10], MIR [2], MIR-RAR, and MIR-mix-RAR methods on the Split-CIFAR10 dataset. Task to classes mapping is as follows: ***Task 1***: *{AIRPL, AUTO}*, ***Task 2***: *{BIRD, CAT}*, ***Task 3***: *{DEER, DOG}*, ***Task 4***: *{FROG, HORSE}*, ***Task 5***: *{SHIP, TRUCK}*.

For case (1), we select all samples from class *Auto* and plot the regions in Fig 7. It is expected that in case of worse forgetting, the decision regions would be dominated by the last task classes even when we use the first task's samples to model the visualization plane. In Fig. 7, the plane is mostly dominated by green (and blue) color in case of ER. In case of MIR-mix-RAR, we see the plane mostly covering the class used to construct the visualization plane, even when the class selected (*Auto*) belongs to the first task the model encountered.

Similarly, in Fig. 8 (case (2)) & 9 (case (3)), as we go from left to right, we see the decision regions being more structured around the classes covered in the triplet set and less dominated by the color of the classes from the last task — this demonstrates that forgetting is minimized when using RAR and mix-RAR.